Cruise ANTARKTIS XII/4 of RV "Polarstern" in 1995: CTD-Report

Jüri Sildam

Ber. Polarforsch. 178 (1995)
ISSN 0176 - 5027

Contents

Introduction

The report presents the results of the CTD measurements carried out in the Bellingshausen Sea - an area rare of CTD measurements. The main part of the report consists of the brief description of the CTD data acquisition and processing routines, the vertical profiles of temperature, salinity and density, and of the plots of the distribution of these properties along the hydrographic sections. The final part of the report deals with the notably similar structure of the vertical density distribution at different locations if presented as a function of a non dimensional vertical co-ordinate. It is pointed out that such a distribution could be an asymptotic limit of stationary mixing along neutral surfaces.

Tab. 1: The list of CTD stations

Station	AWI-No	Date	Start (UTC)	Max depth (UTC)	Latitude Deg. min	Longitude Deg. min	Water Depth	Meas. Depth
001		23.03.95	01:00	01:31	51°37,0'S	80 39,8W	4155	2001
002		23.03.95	05:38	06:14	51°29,3'S	81°25,6'W	4340	2001
003		23.03.95	09:42	10:17	51°21,9'S	82°12,5'W	4368	2000
005		23.03.95	21:00	21:49	51°13,5'S	82°58,7'W	4396	1970
006		24.03.95	01:54	02:29	51°06,1'S	83°44,8'W	4468	1977
007		24.03.95	06:26	07:02	50°58,1'S	84°30,7'W	4512	1977
008		24.03.95	11:16	11:51	50°48,5'S	85°24,5'W	4377	1985
010		24.03.95	21:39	22:15	50°42,6'S	86°01,5'W	4573	1985
011		25.03.95	04:17	04:52	50°34,2'S	86°49,5'W	4613	1984
012		25.03.95	08:31	09:06	50°25,5'S	87°36,7'W	4690	2013
013		25.03.95	12:36	13:10	50°17,6'S	88°24,9'W	4614	1976
014	PS2660-6	26.03.95	01:26	02:59	50°08,4'S	89°14,1'W	4997	4997
017		26.03.95	16:56	17:30	50°39,0'S	89°15,6'W	4608	1974
019		26.03.95	20:54	21:29	51°09,1'S	89°18,8'W	4637	1988
021	PS2661-5	27.03.95	05:54	07:21	51°24,6'S	89°20,5'W	4724	4724
023		27.03.95	13:19	13:55	51°54,7'S	89°24,7'W	4830	1975
026		27.03.95	17:56	18:32	52°24,5'S	89°26,9'W	4905	1974
028	PS2662-1	27.03.95	21:51	23:22	52°53,7'S	89°29,5'W	4937	4937
030		28.03.95	05:03	05:39	53°24,3'S	89°33,7'W	4941	1977
032	PS2664-5	29.03.95	03:56	04:34	53°49,1'S	89°34,8'W	4810	1974
037		29.03.95	08:05	08:58	54°19,2'S	89°38,5'W	4713	2956
045		30.03.95	01:26	02:07	55°28,0'S	89°45,5'W	5121	2000
047	PS2667-7	30.03.95	19:37	21:12	55°39,6'S	89°49,0'W	5510	5449
055	PS2675-1	03.04.95	23:35	01:05	57°52,9'S	93°30,7'W	4917	4857
060	PS2678-6	06.04.95	18:09	19:41	61°30,0'S	97°40,6'W	5211	5211
080	PS2682-1	09.04.95	04:03	04:16	66°31,0'S	97°25,9'W	4734	593
091	PS2683-1	09.04.95	18:22	18:43	68°31,2'S	97°10,0'W	4526	984
103	PS2684-2	12.04.95	01:47	03:09	69°24,9'S	95°01,2'W	4230	4230
104	PS2685-1	12.04.95	16:41	16:54	69°25,1'S	94°10,3'W	3638	587
135	PS2686-3	18.04.95	01:43	02:55	68°17,1'S	89°35,7'W	3920	3920
138	PS2687-1	20.04.95	01:40	03:08	67°58,8'S	92°38,6'W	4466	4466
141	PS2688-5	21.04.95	02:21	02:37	67°13,1'S	91°49,6'W	4616	591
154	PS2692-5	22.04.95	15:40	17:15	65°08,4'S	90°41,4'W	4673	4673
162	PS2696-5	26.04.95	00:22	01:48	63°58,7'S	89°32,0'W	4767	4767
166	PS2697-9	27.04.95	01:45	03:12	63°01,6'S	89°33,9'W	4782	4782
172		28.04.95	02:04	02:51	62°02,6'S	89°30,1'W	4864	1964
177	PS2699-1	28.04.95	09:56	11:32	61°01,1'S	89°30,0'W	4957	4957
182	PS2700-4	29.04.95	07:29	09:09	60°16,2'S	89°31,0'W	5020	5020
186	PS2701-3	30.04.95	02:47	03:25	59°27,0'S	89°31.0W	4789	1973
207	PS2714-5	09.05.95	08:55	10:40	57° 26,5S	89 16,3W	5104	5104

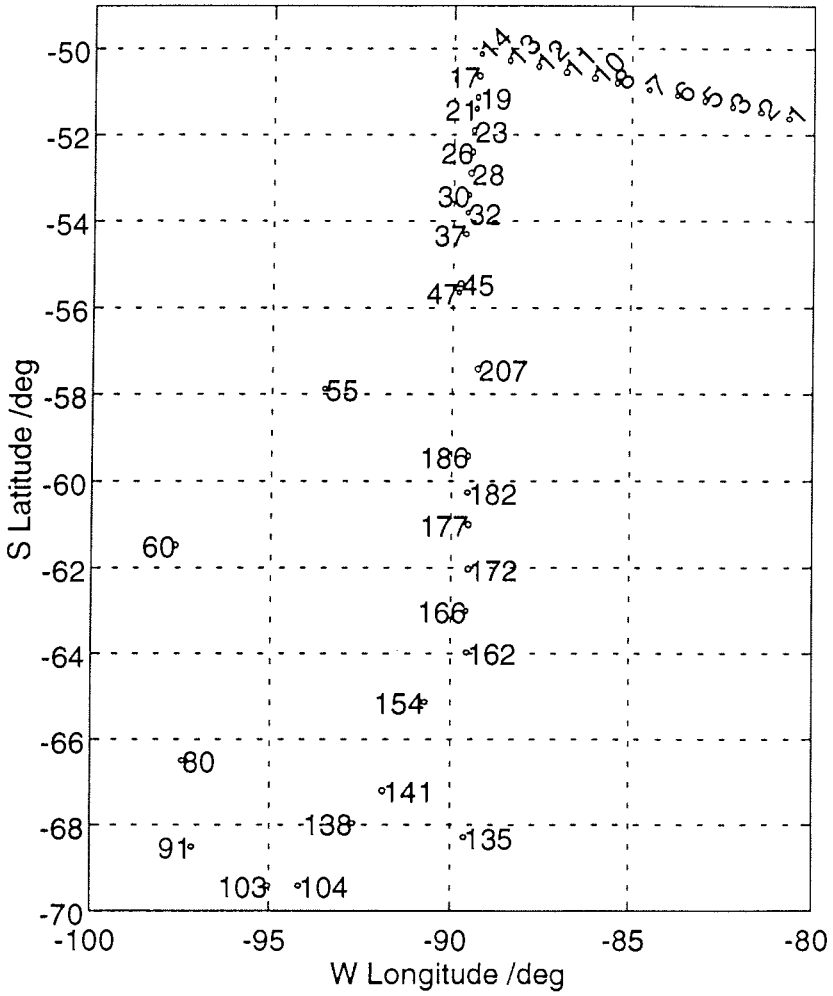

Figure 1. Positions of CTD stations during ANTXII/4 cruise of R/V "Polarstern".

Instrumentation

Hydrographic casts were occupied by 24 - place General Oceanic Rosette equipped with 12 - litre bottles and Sea-Bird 911 *plus* (SB) CTD. SB had a single temperature (pressure protected thermistor), a Paroscientific Digiquartz pressure and a conductivity sensor. Flow pumped at a constant rate via TC duct ensured that the conductivity and temperature sensors measured the same water with a fixed time difference. Initial accuracies of measurements as provided by SB specifications were for conductivity 0.0003 S/m, for temperature 0.002 °C and for pressure 0.015% of full scale (here 6800 dbar). The temperature and conductivity sensors were calibrated prior to and after the cruise. Checks of CTD temperature and salinity values versus reversing thermometers and salinity bottle values (analysed on Guidline Autosal 8400 salinometer) respectively were performed at the deep CTD stations.

Data Processing

Data acquisition and processing was carried out according to standard routines of Sea Bird 9/11 CTD data processing. It consisted of the following steps: 1) converting of the raw data to pressure, temperature (IPTS-68) and conductivity; 2) aligning of conductivity relative to pressure by -0.01 seconds which was determined on the basis of experience from previous cruises (*Budéus* 1995, personal communication); 3) conductivity cell thermal mass correction (alpha=0.03 and 1/beta=9.0); 4) low pass filtering of pressure with a time constant of 0.15 seconds; 5) removal of the scans where the CTD was travelling backwards; 5) averaging of data into 2 dbar bins. Finally, salinity (PSS-78) and density were calculated.

Comparison of the CTD temperature with the reversing thermometers showed that the differences at the deep stations did not exceed the accuracy of the reversible thermometers i.e. 0.002 °C. Comparison of the pre- and postcruise calibration results showed that drift of the temperature sensor between the two calibrations carried out in March 02 and July 29, was less than 0.001 °C. So, no corrections for temperature measurements were introduced.

Comparison of the CTD salinity measurements with the salinity bottle values, taken at the deep stations showed the existence of a mean shift of 0.0033 with the higher values of the bottle salinities. No statistically significant time trend was observed. Introducing the postcruise calibration slope with the precruise calibration coefficients resulted in the increase of salinity of the CTD data on an average by 0.0034. Thus salinity was calculated using the precruise calibration

coefficients and the slope determined from the postcruise calibration as suggested by an application note of SBE.

4 CTD Profiles

On the following pages the CTD profiles from all hydrographic stations are displayed. To provide the possibility of comparision of the profiles with each other, the same scale has been used for all profiles. For this reason, the shallow CTD casts (200-600 m) that have been carried out additionally to the deep ones at some stations to satisfy the water requirement of the different groups are not shown in the present report.

Station: 1 ANT XII/4 1995

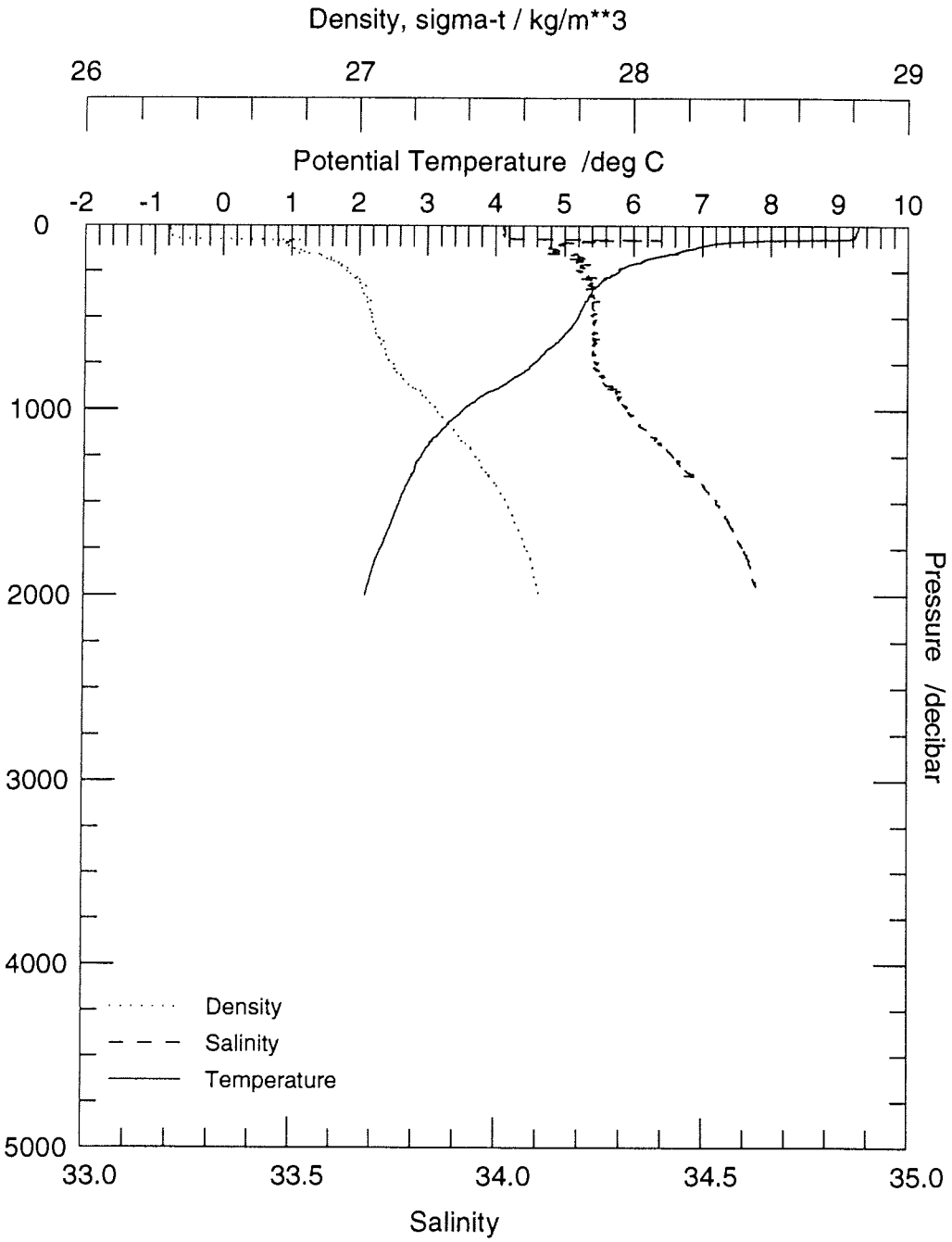

Station: 2 ANT XII/4 1995

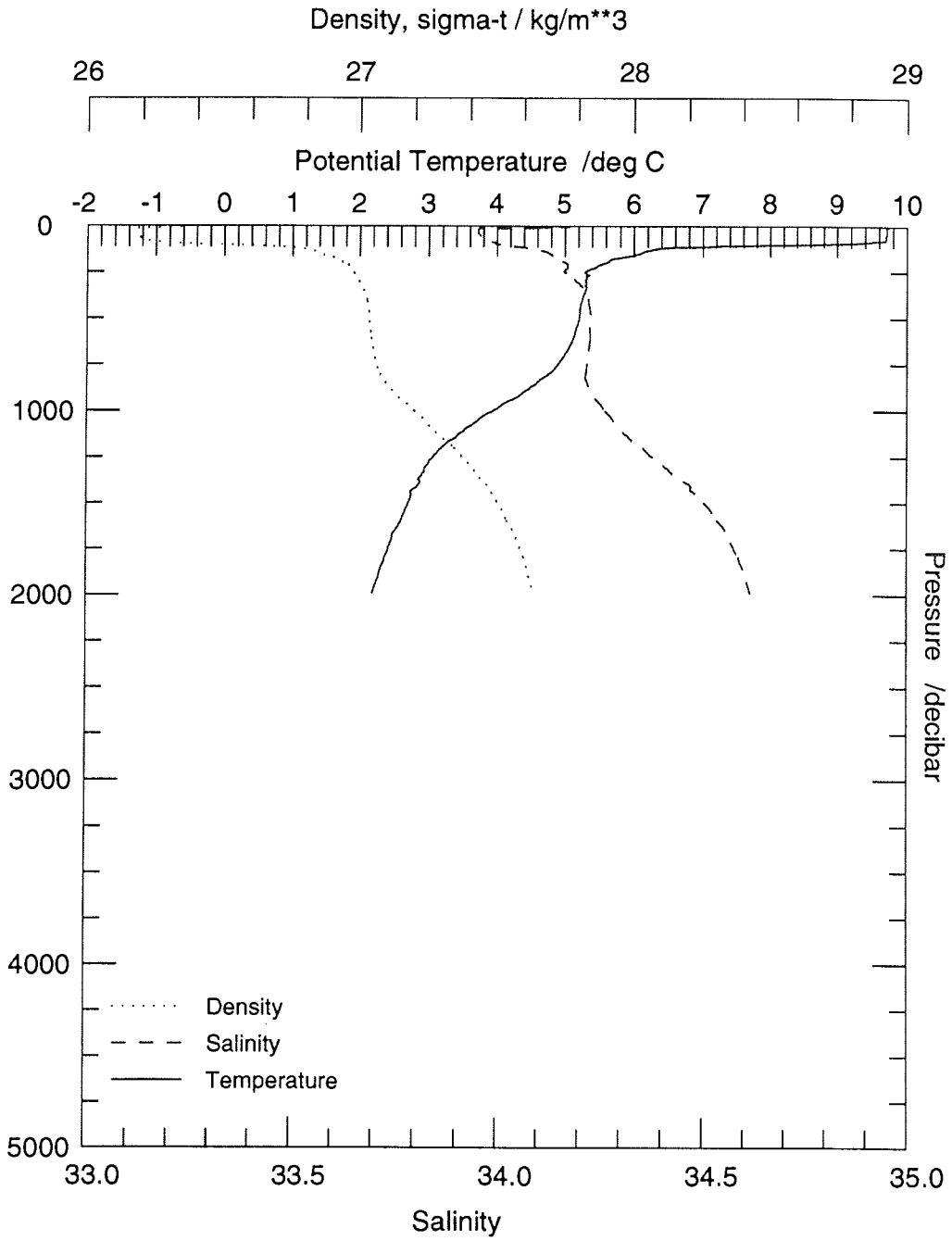

Station: 3 ANT XII/4 1995

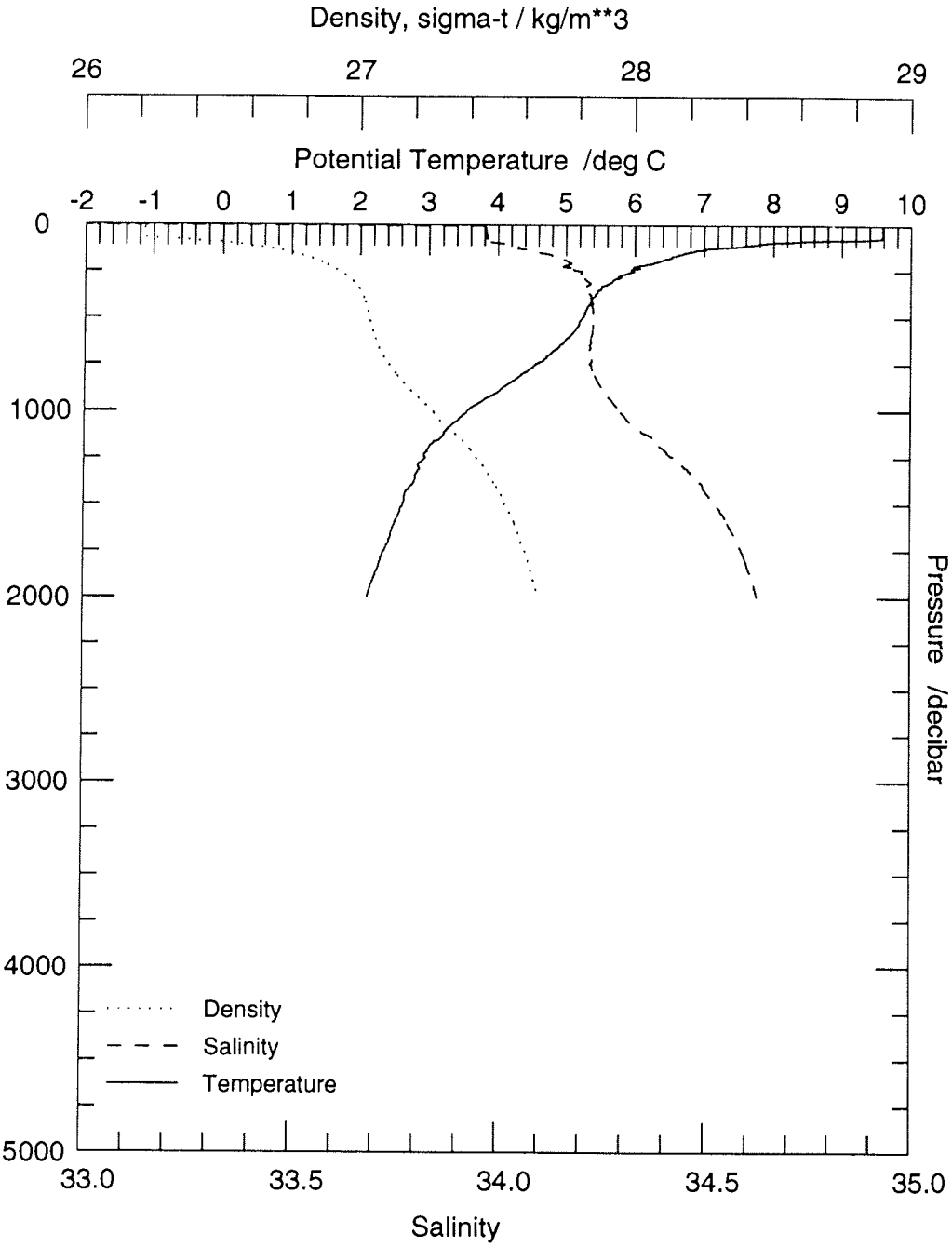

Station: 5 ANT XII/4 1995

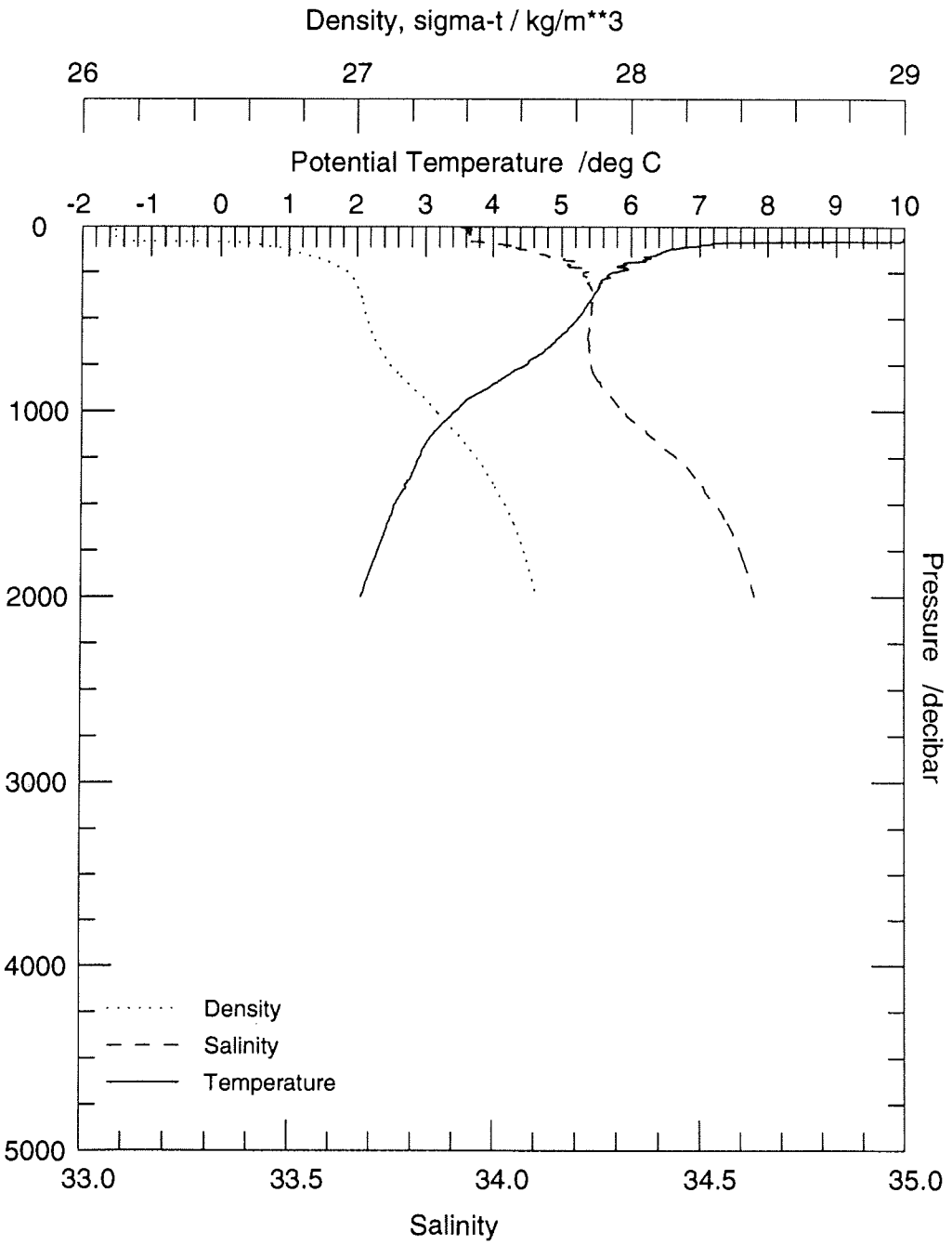

Station: 6 ANT XII/4 1995

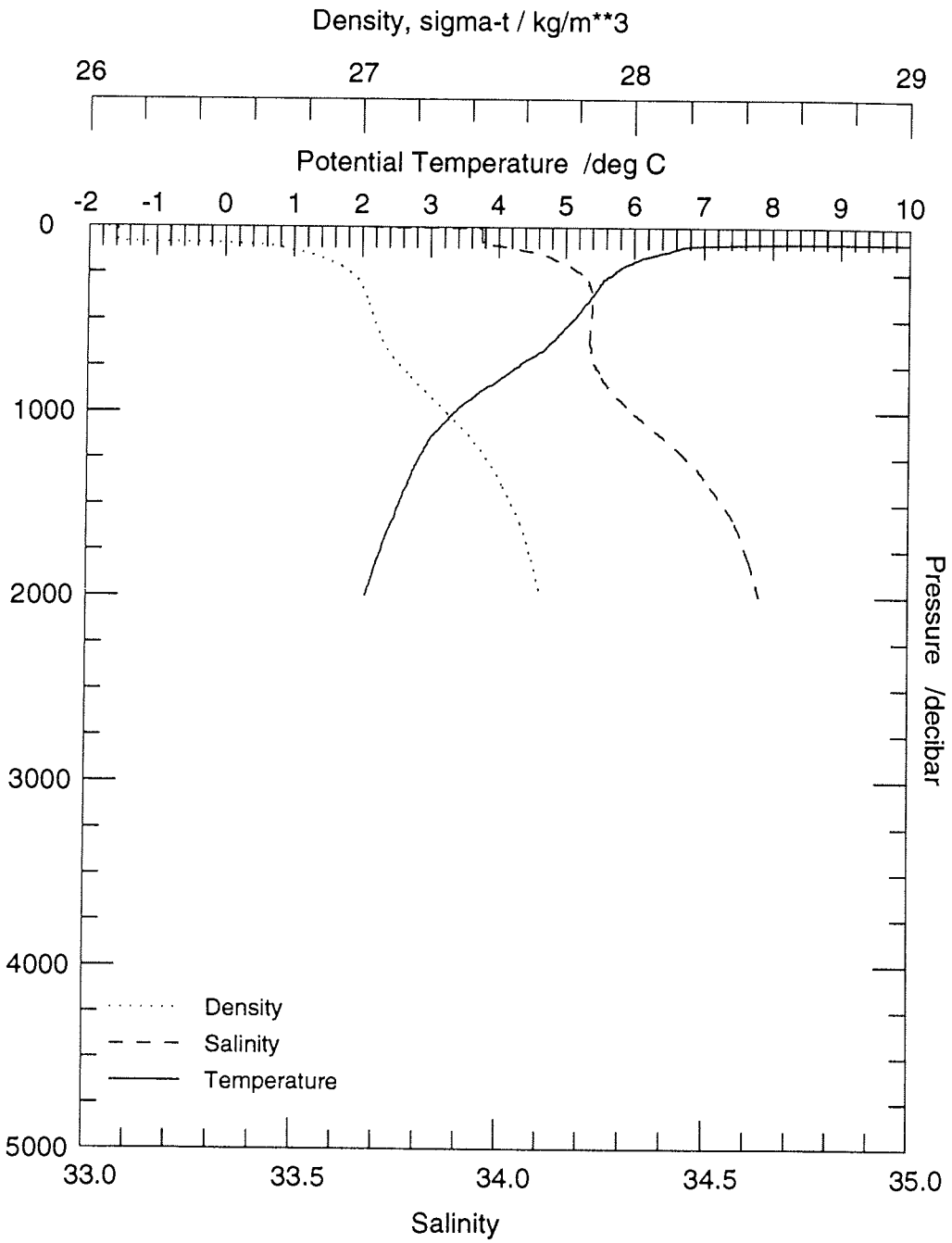

Station: 7 ANT XII/4 1995

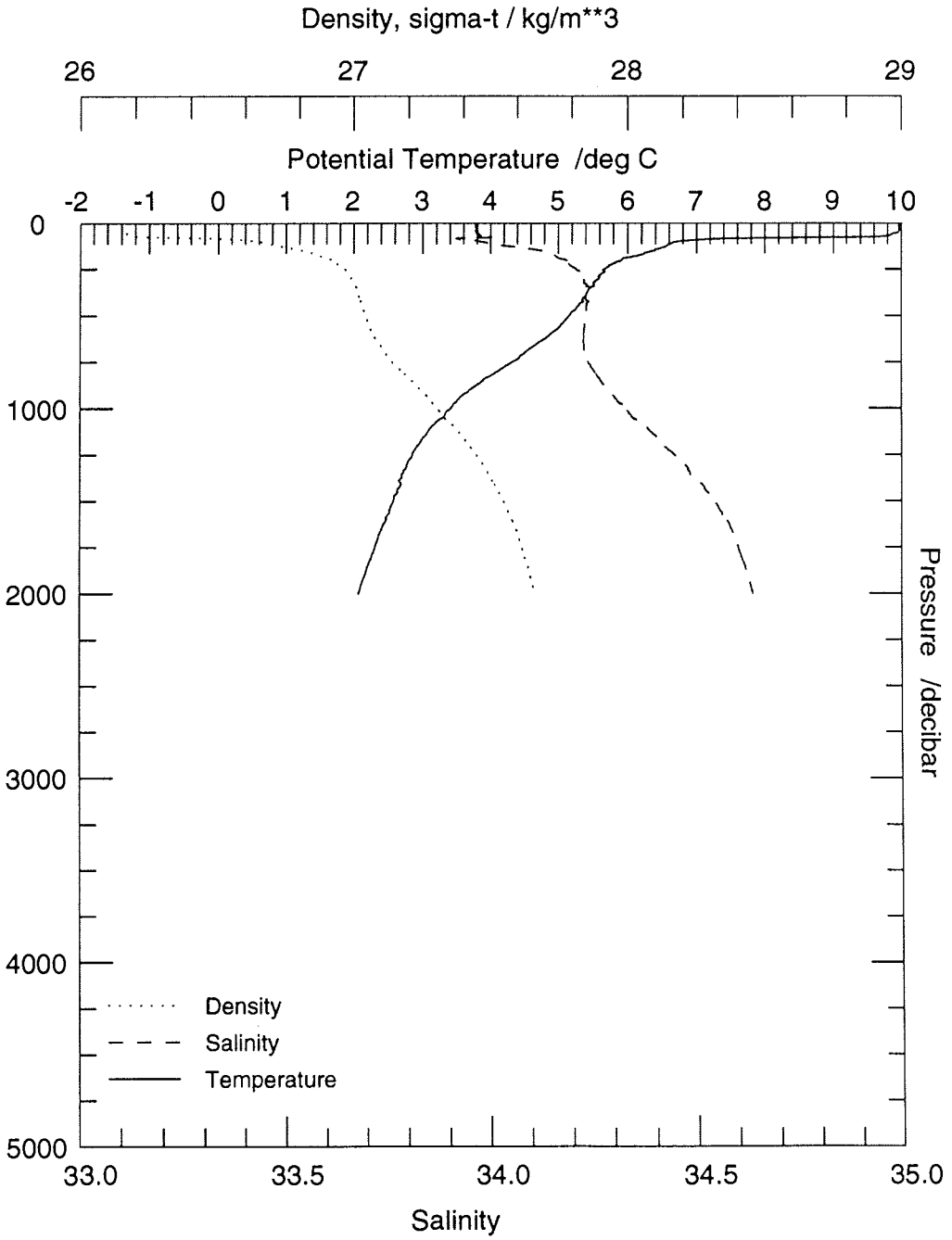

Station: 8 ANT XII/4 1995

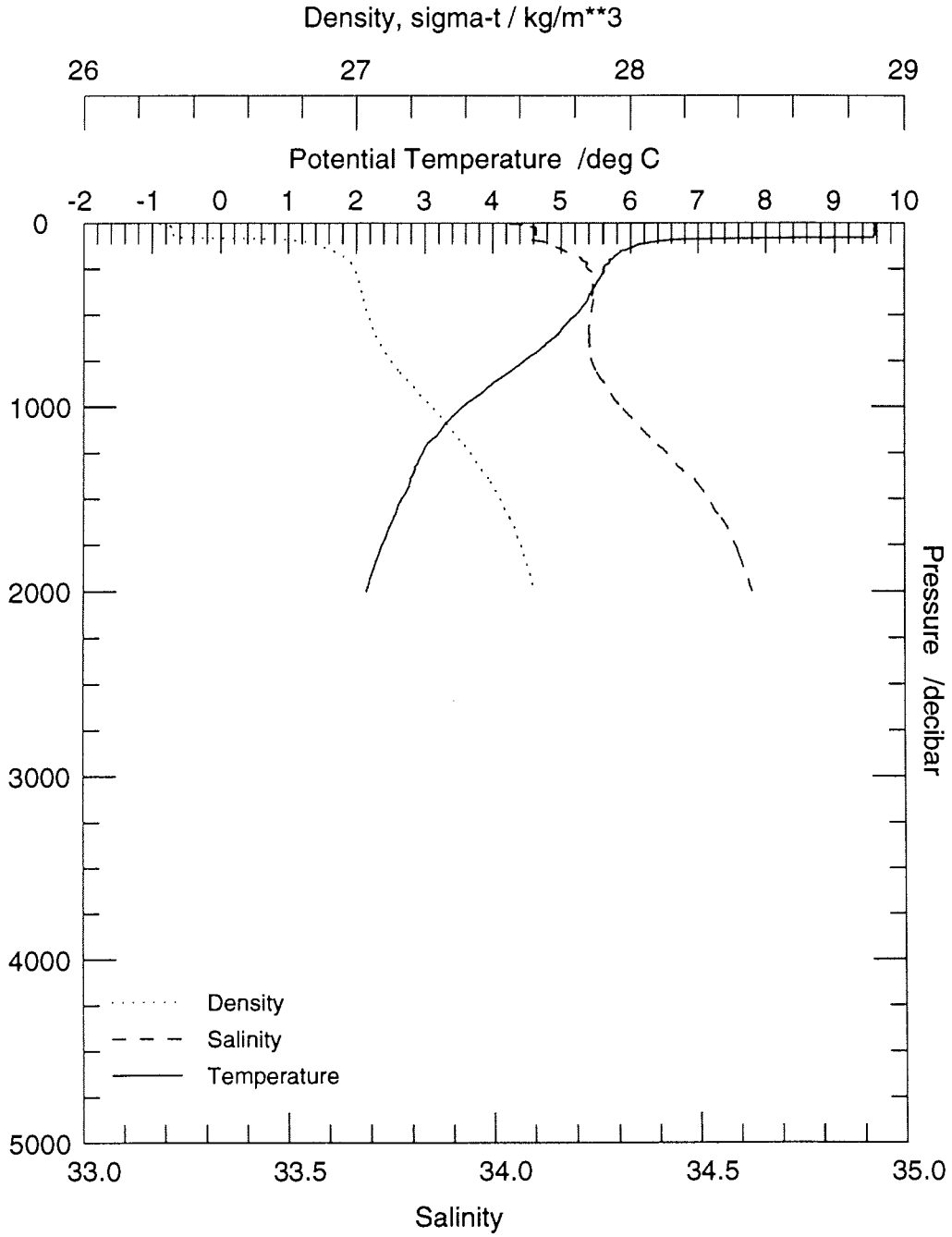

Station: 10 ANT XII/4 1995

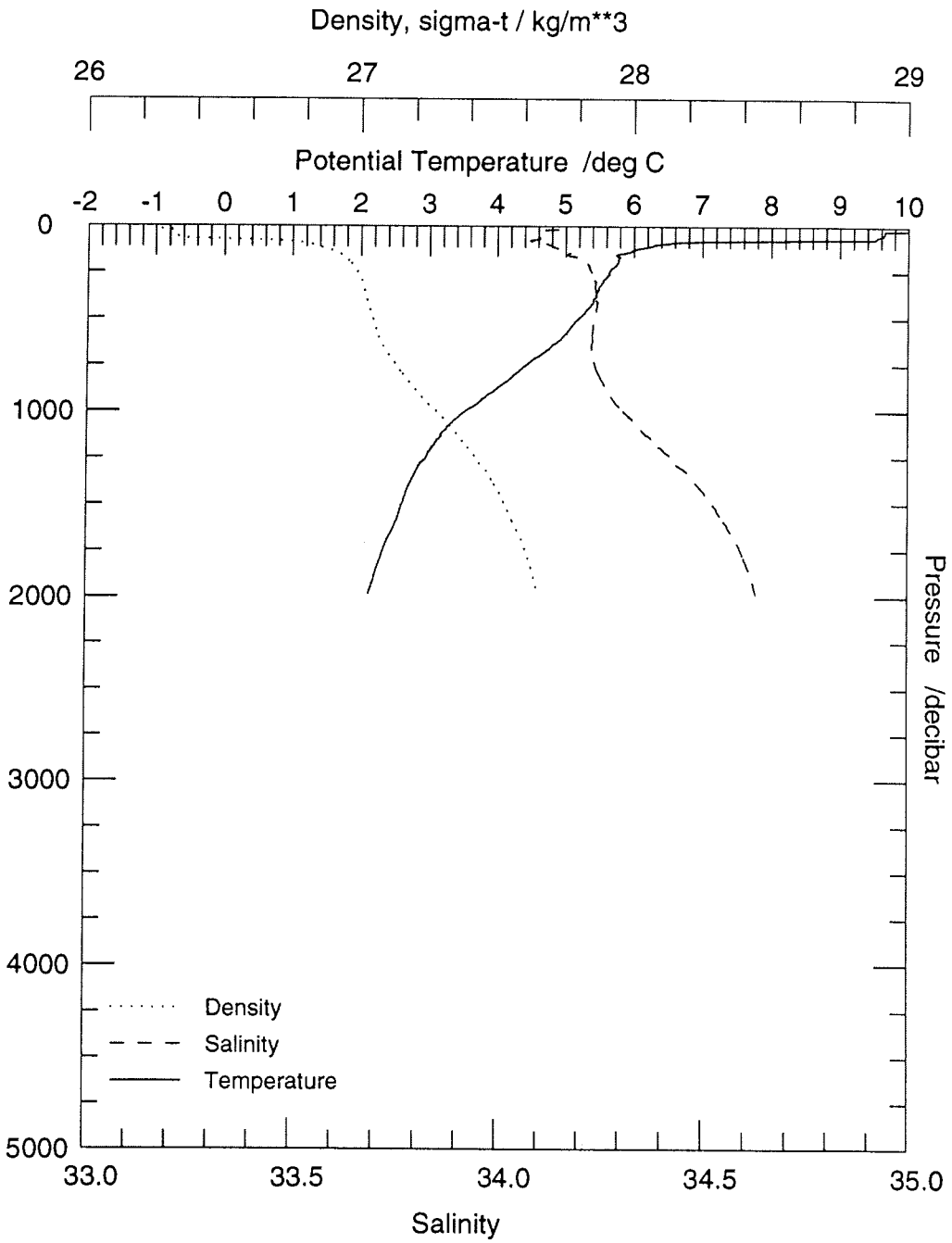

Station: 11 ANT XII/4 1995

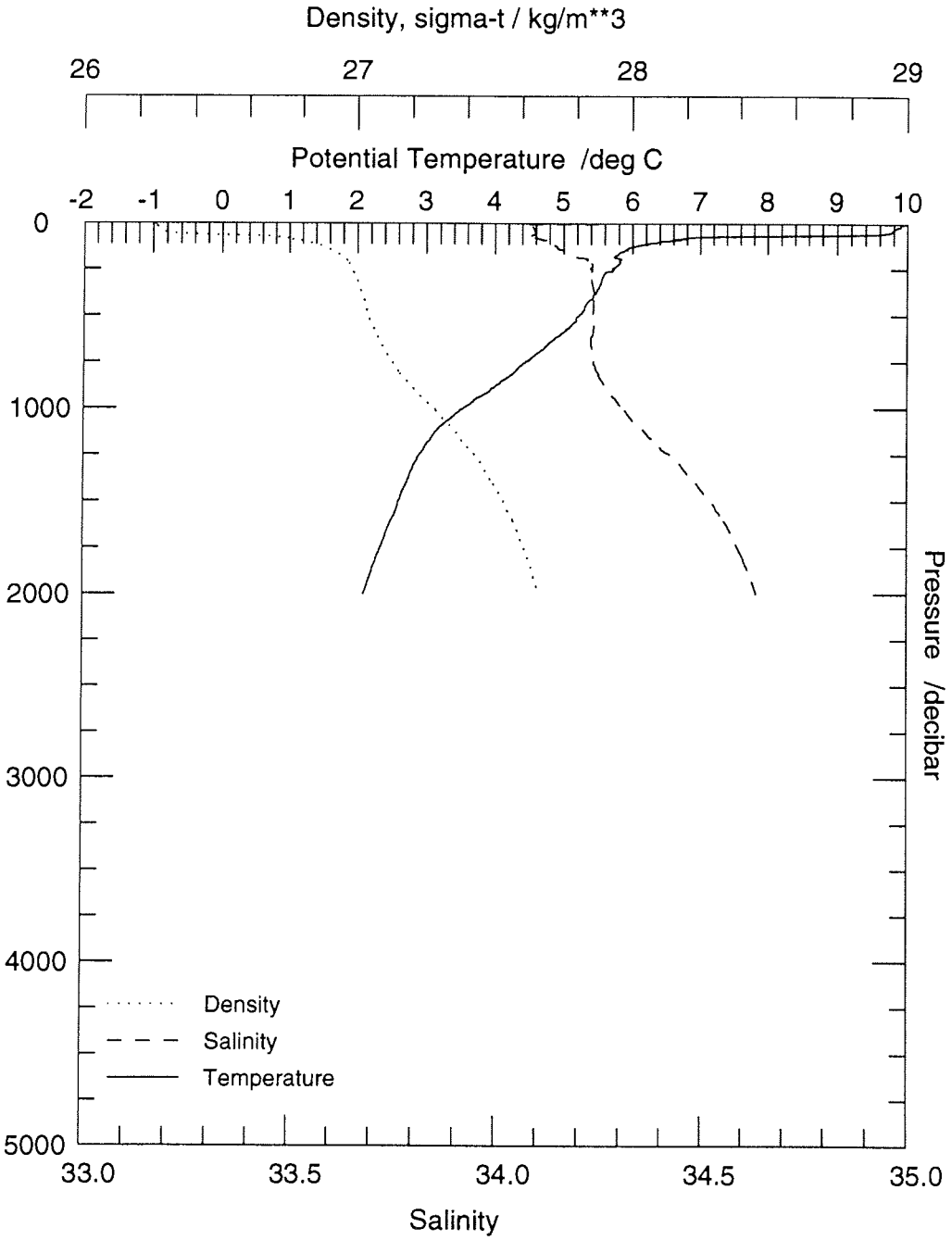

Station: 12 ANT XII/4 1995

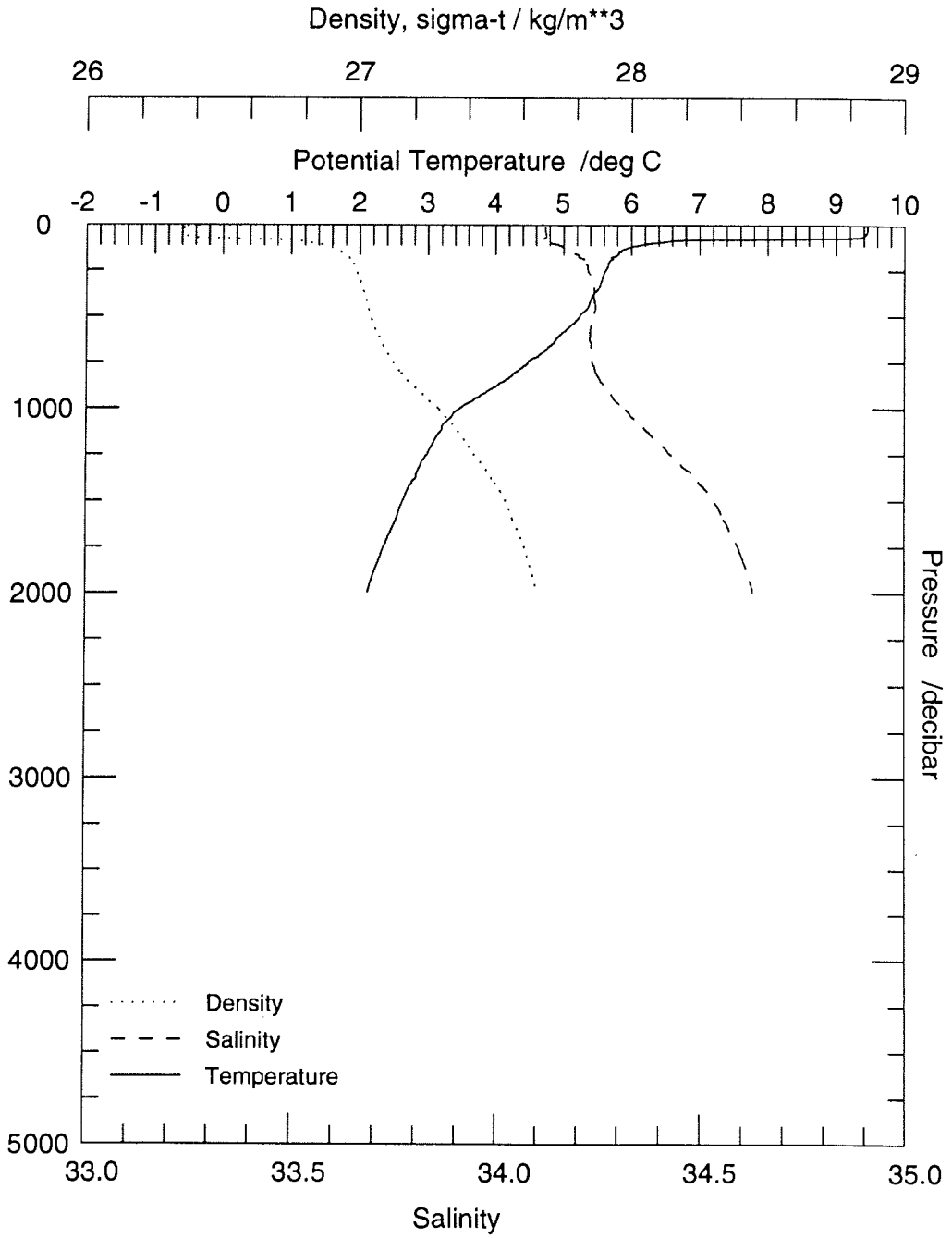

Station: 13 ANT XII/4 1995

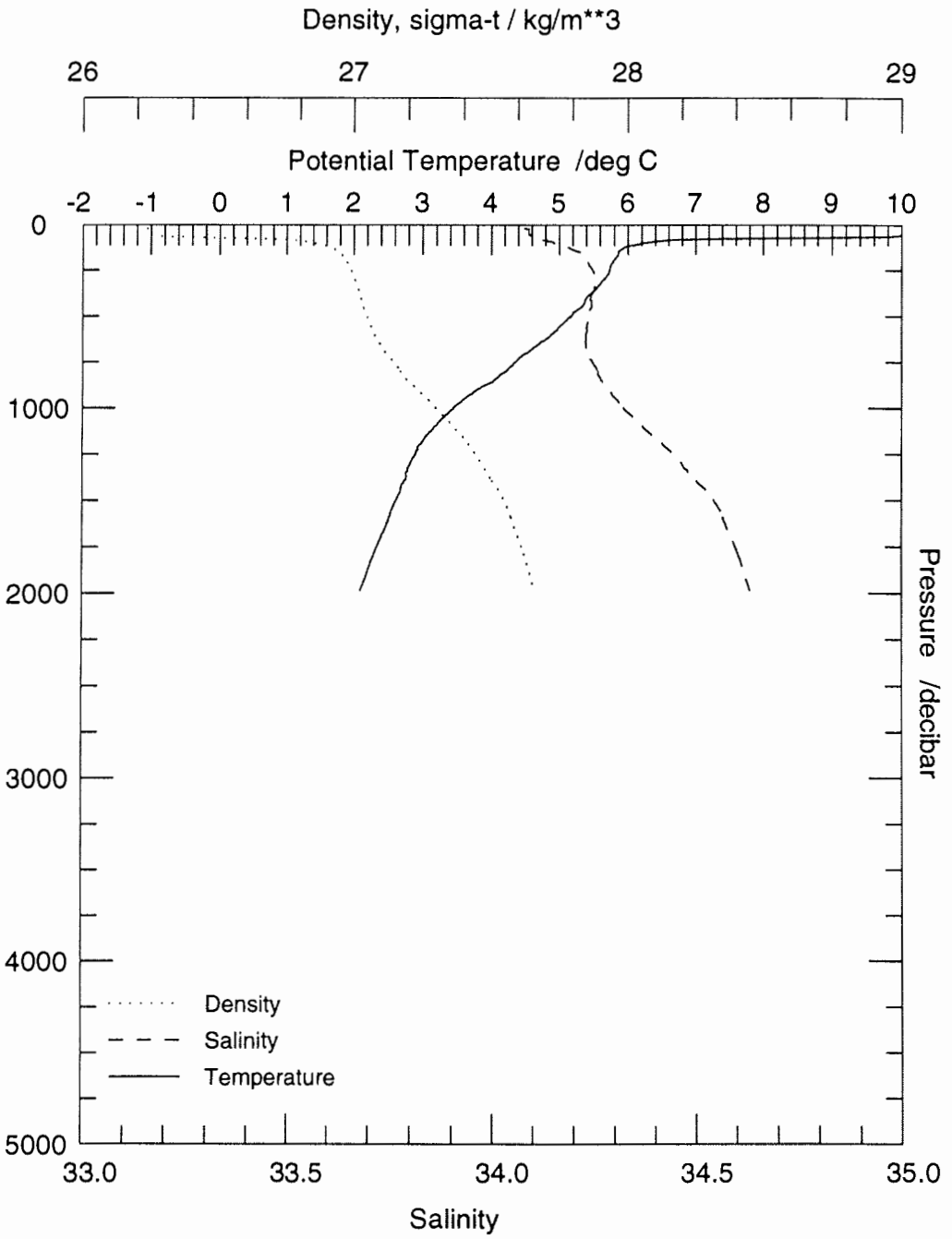

Station: 14 ANT XII/4 1995

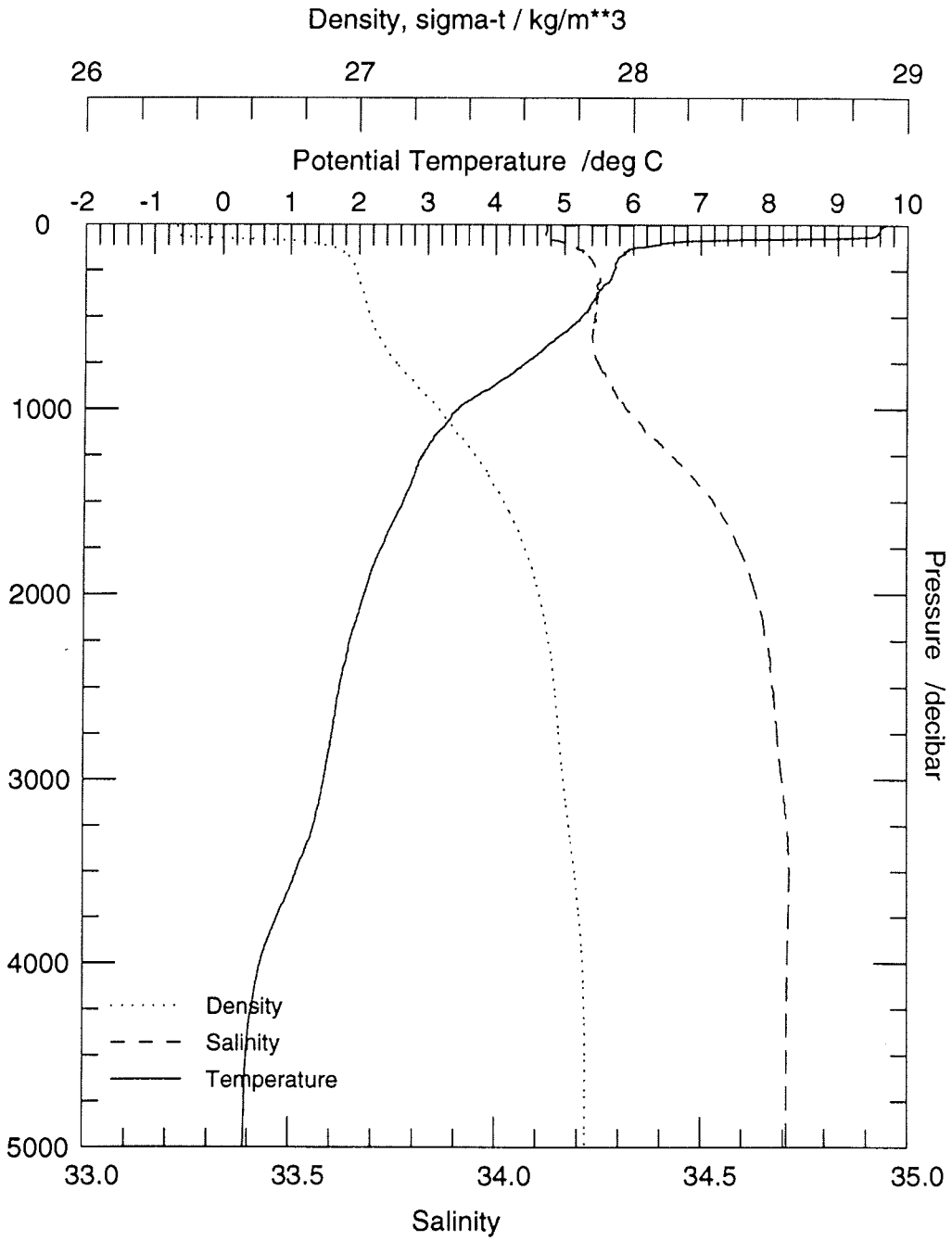

Station: 17 ANT XII/4 1995

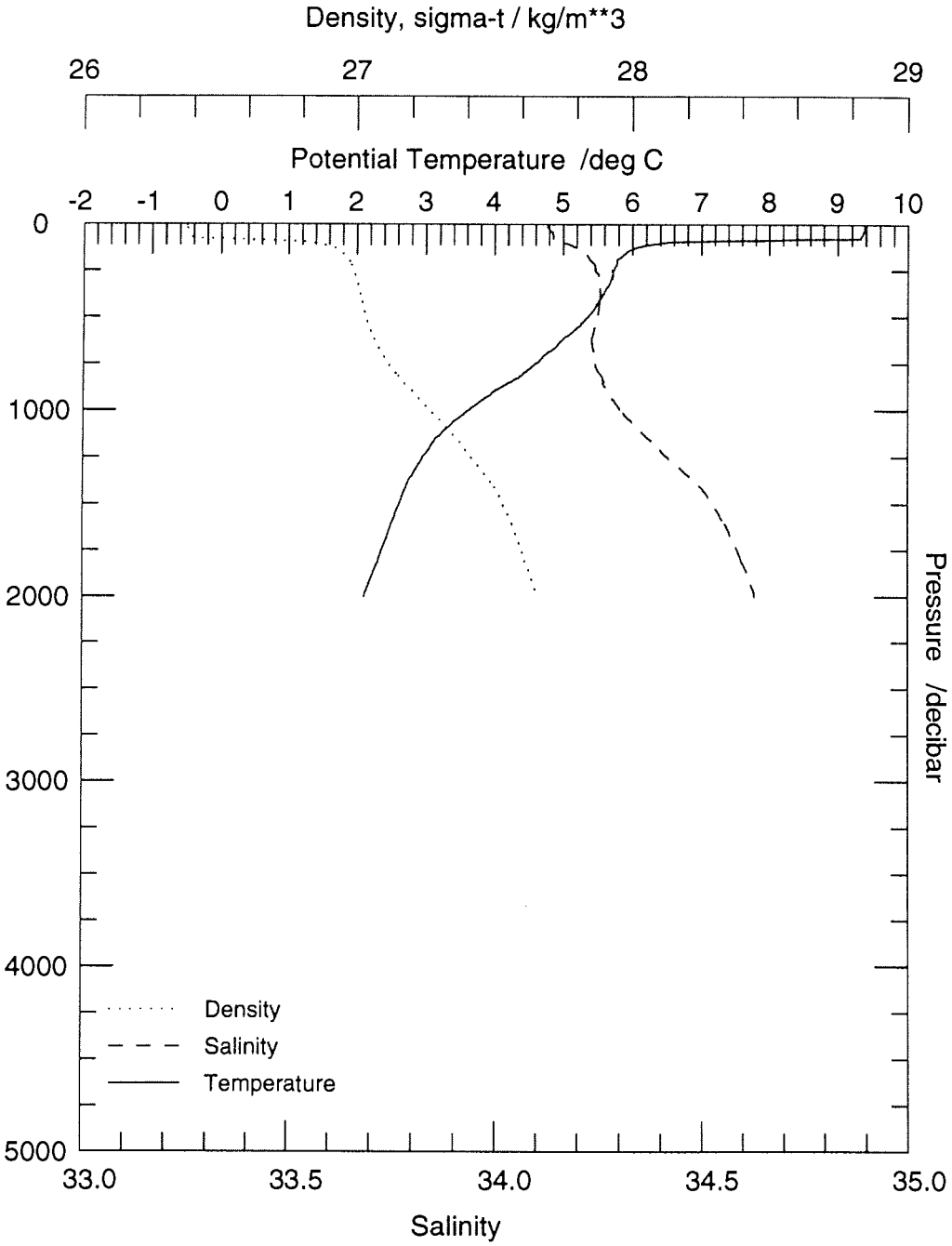

Station: 19 ANT XII/4 1995

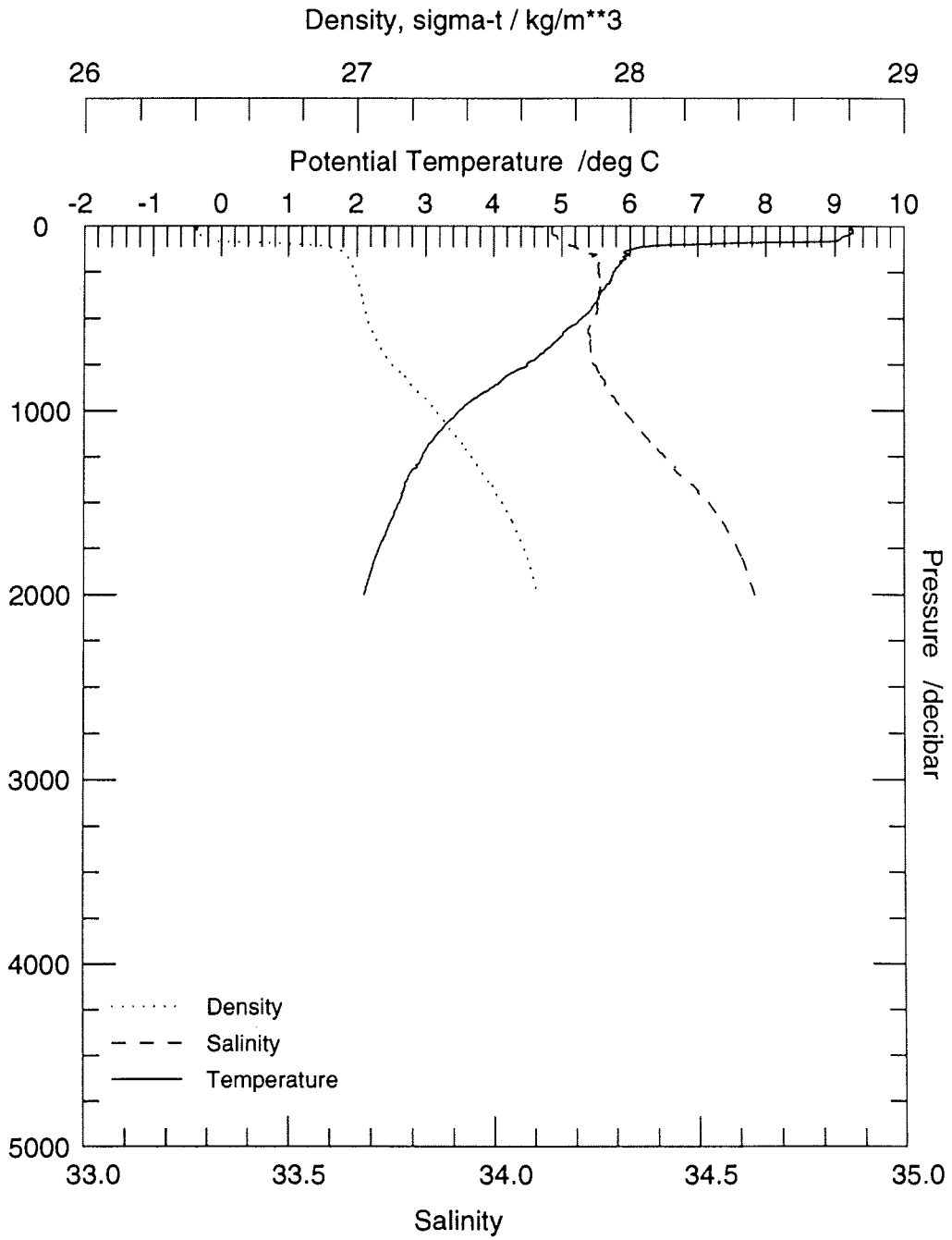

Station: 21 ANT XII/4 1995

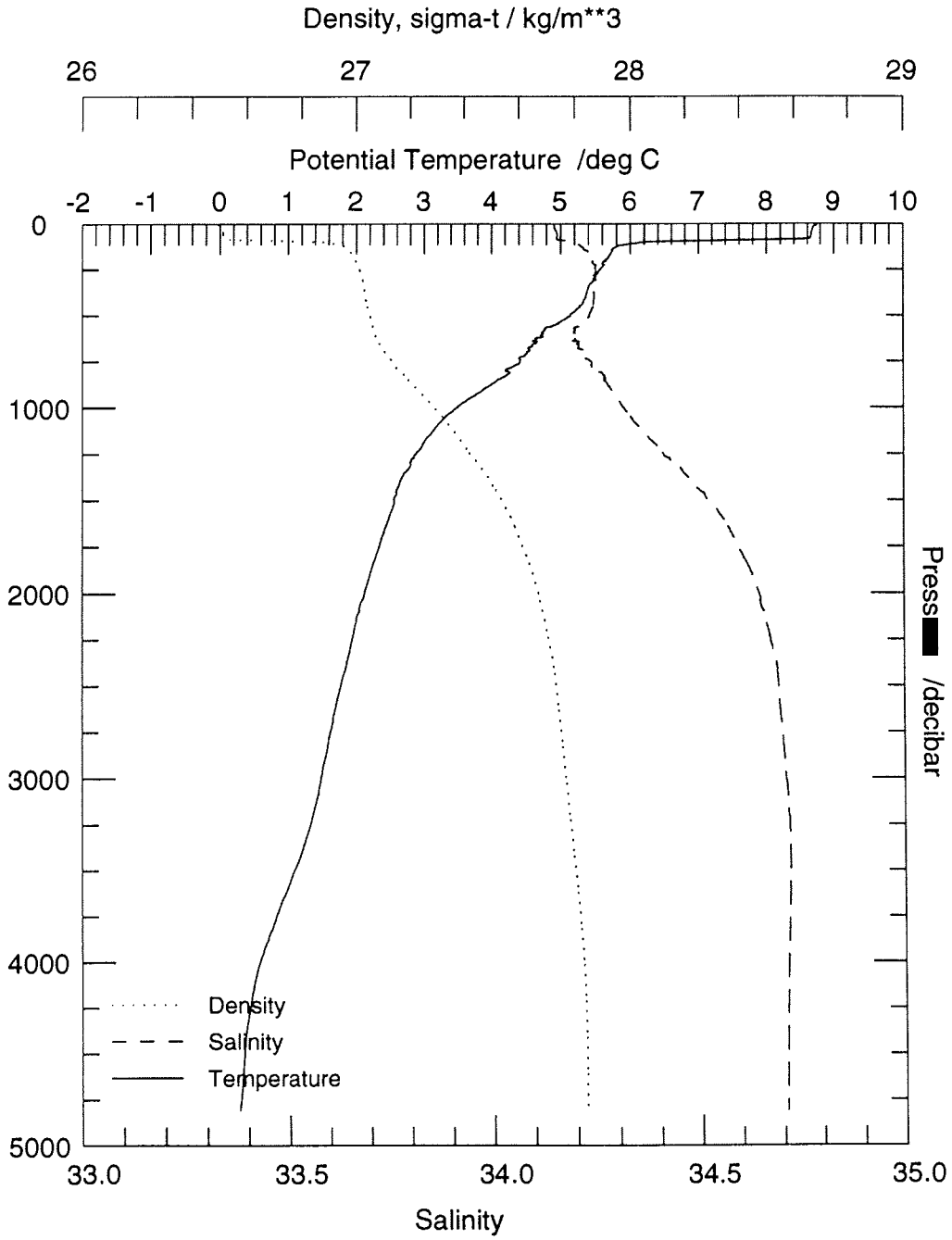

Station: 23 ANT XII/4 1995

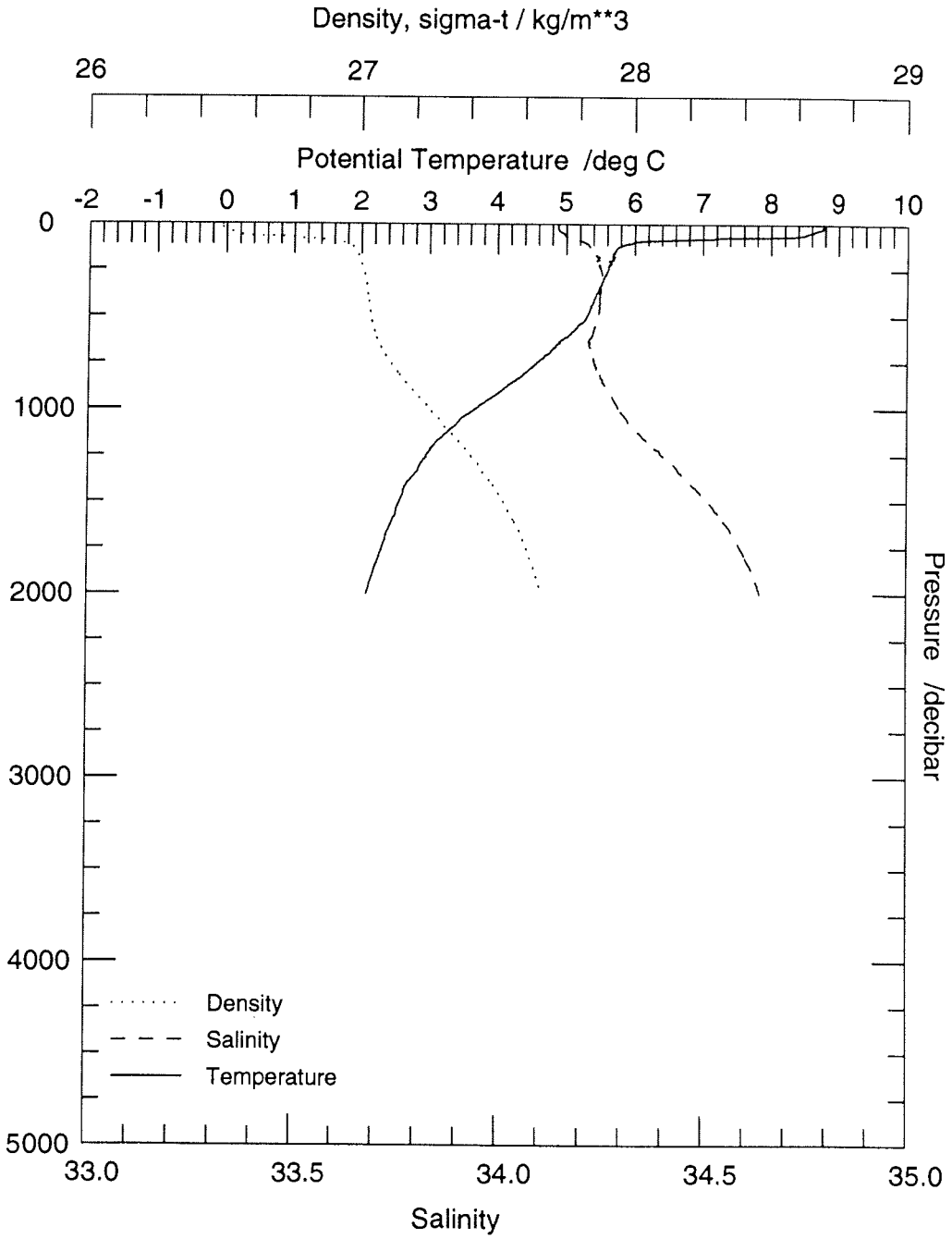

Station: 26 ANT XII/4 1995

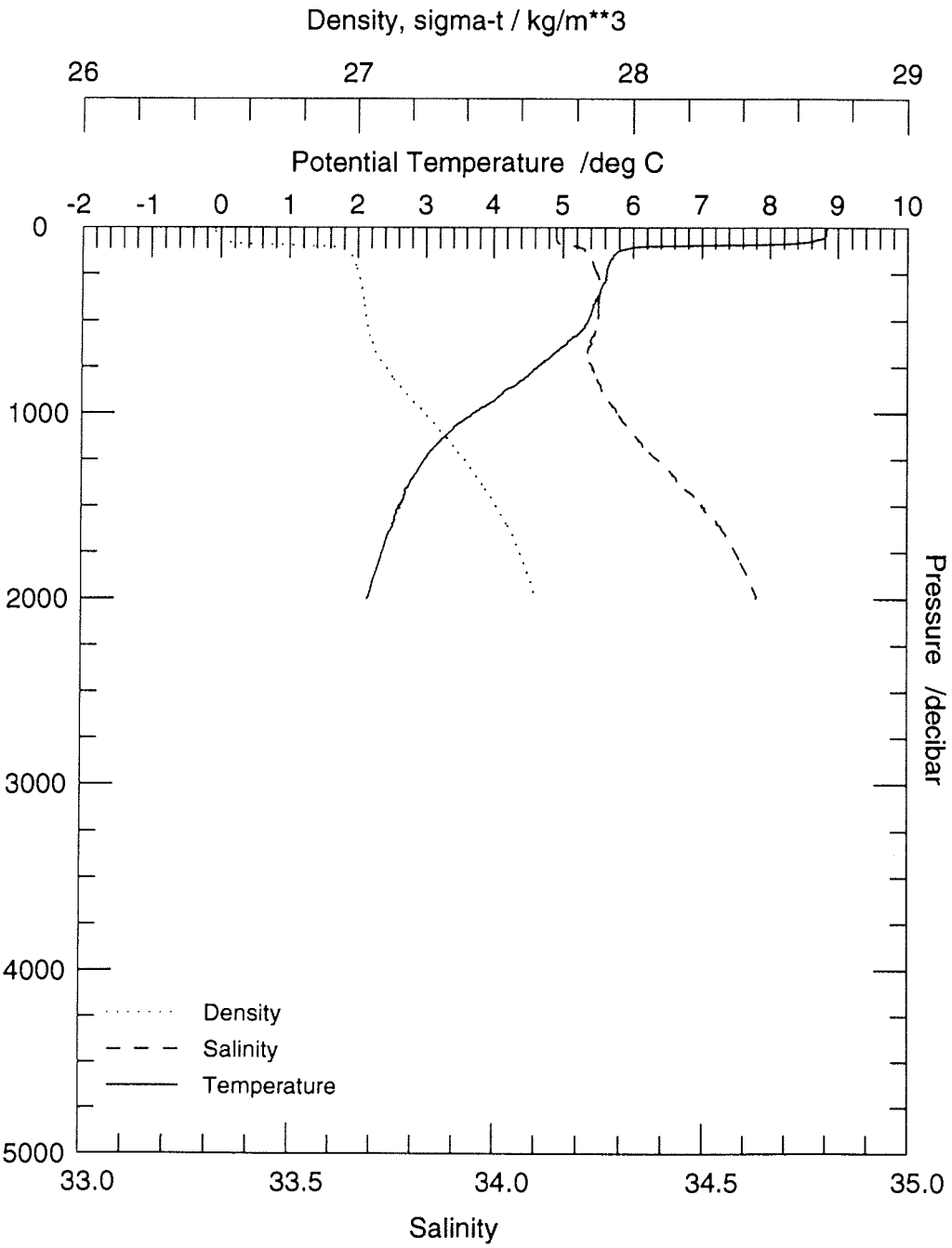

Station: 28 ANT XII/4 1995

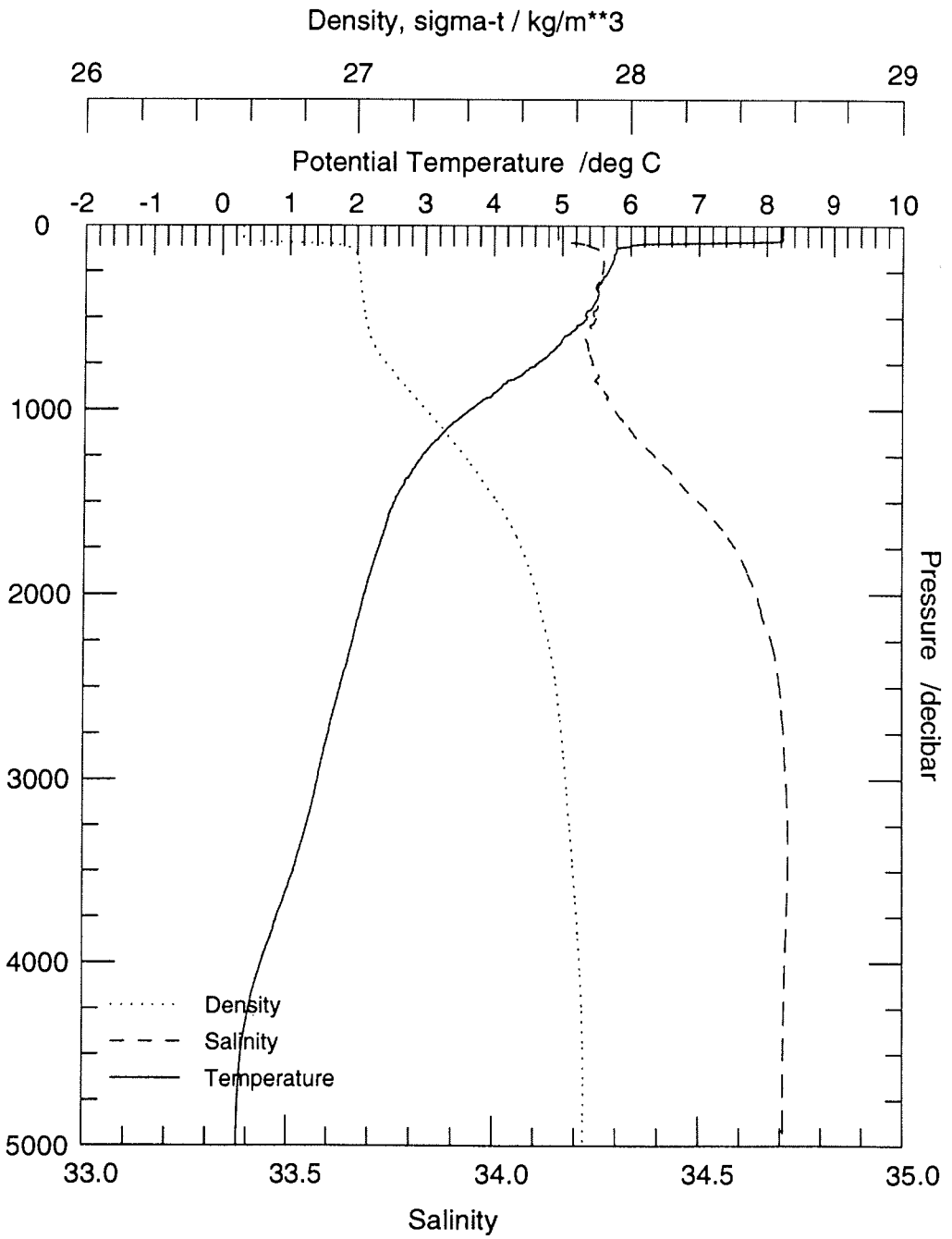

Station: 30 ANT XII/4 1995

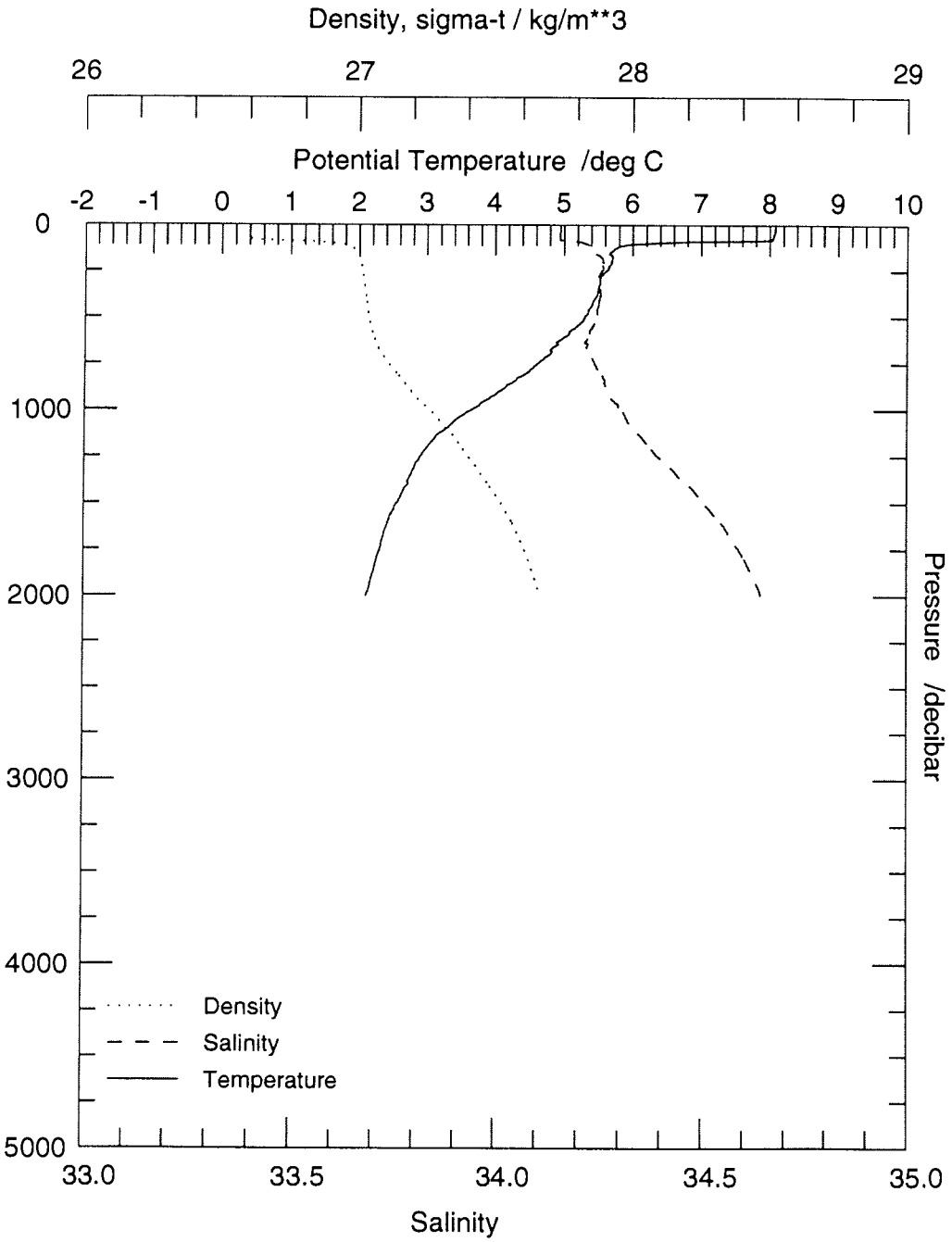

Station: 32 ANT XII/4 1995

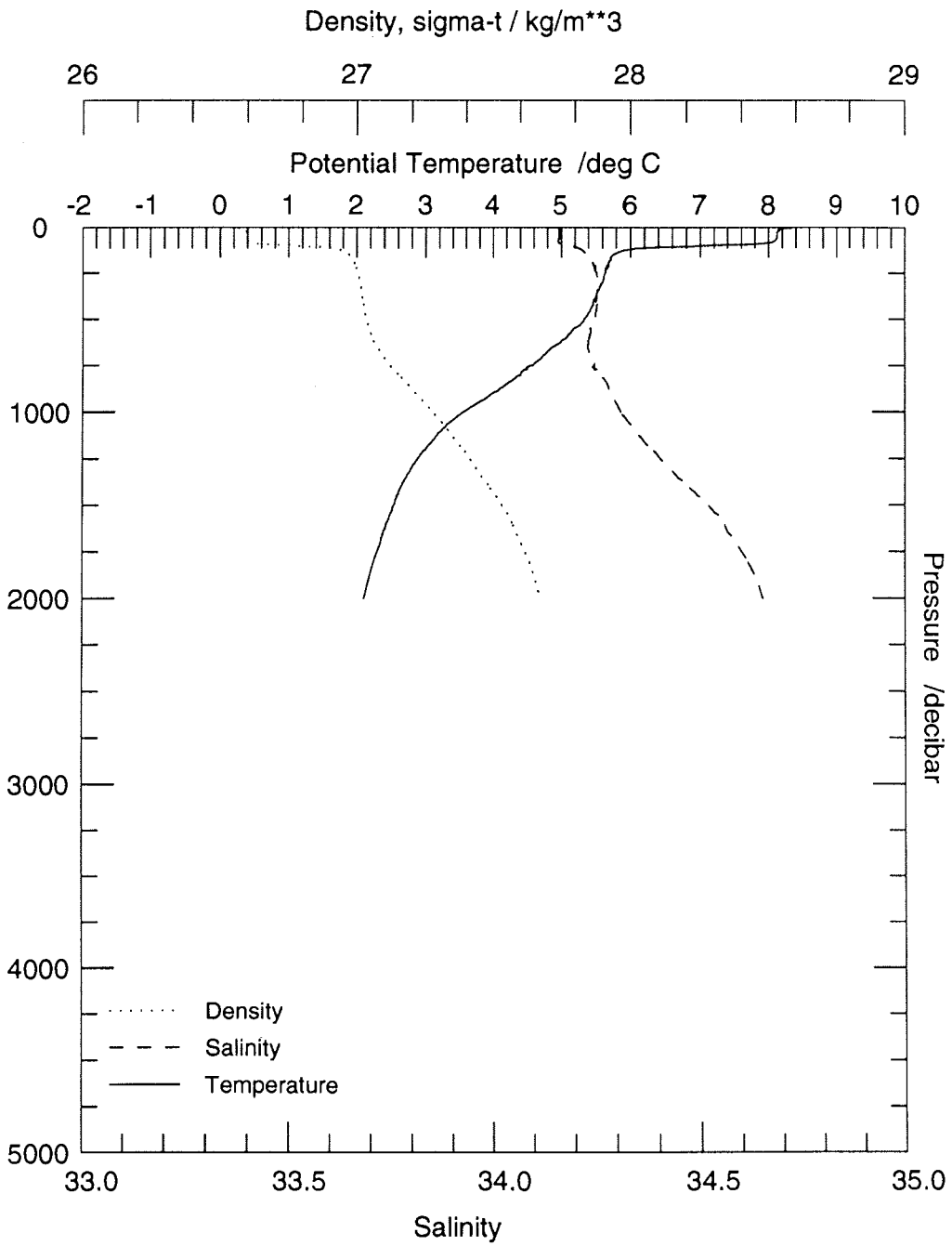

Station: 37 ANT XII/4 1995

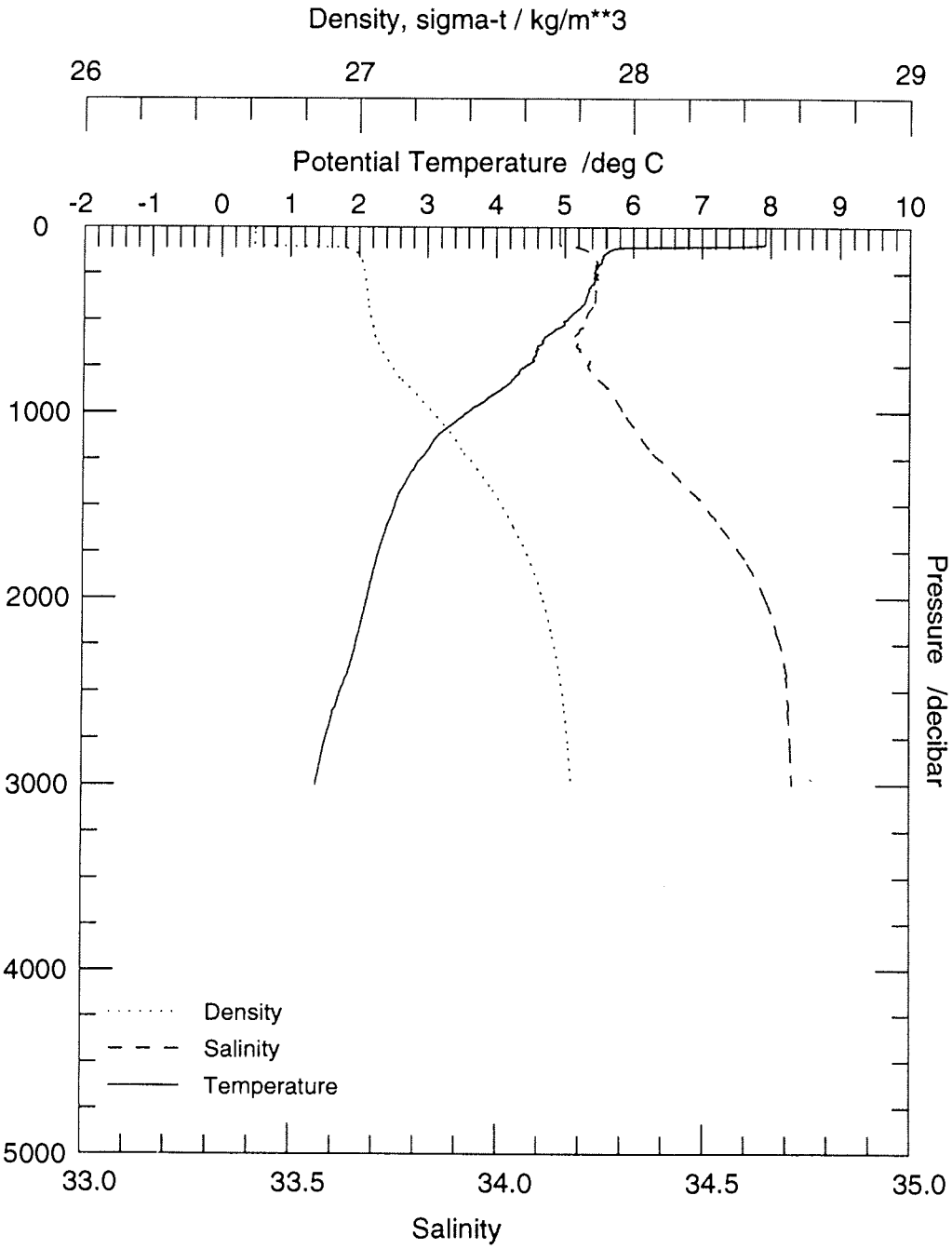

Station: 45 ANT XII/4 1995

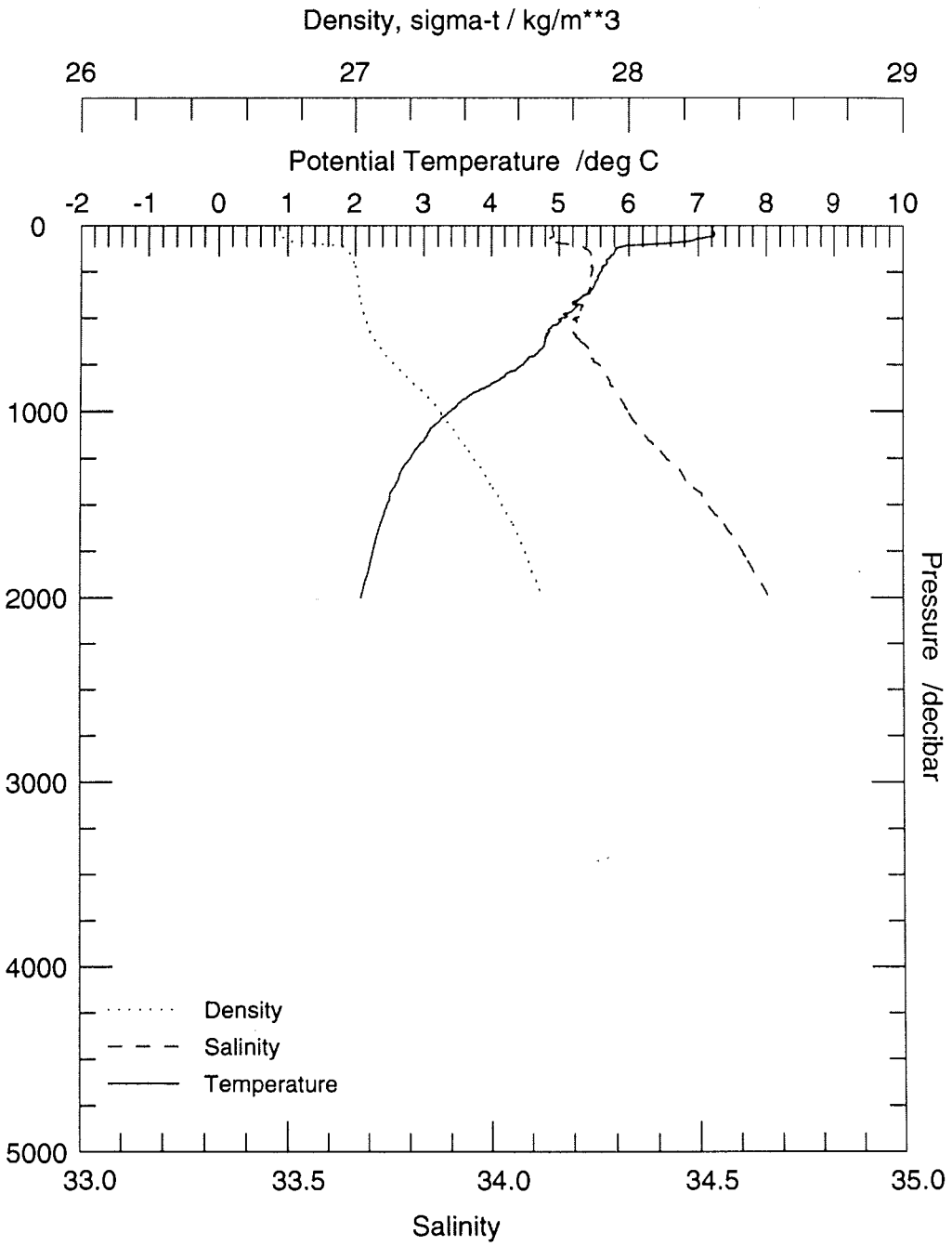

Station: 47 ANT XII/4 1995

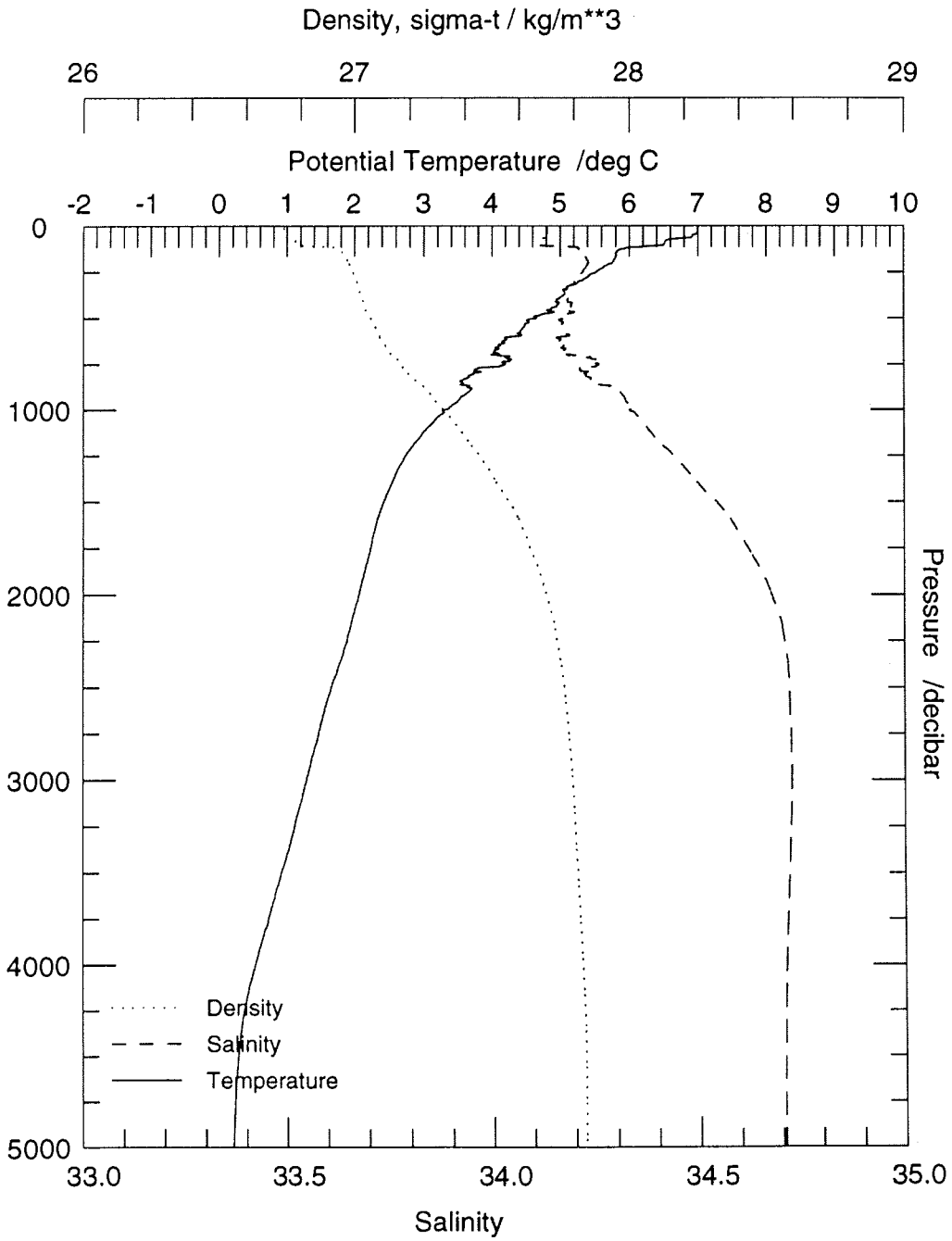

Station: 55 ANT XII/4 1995

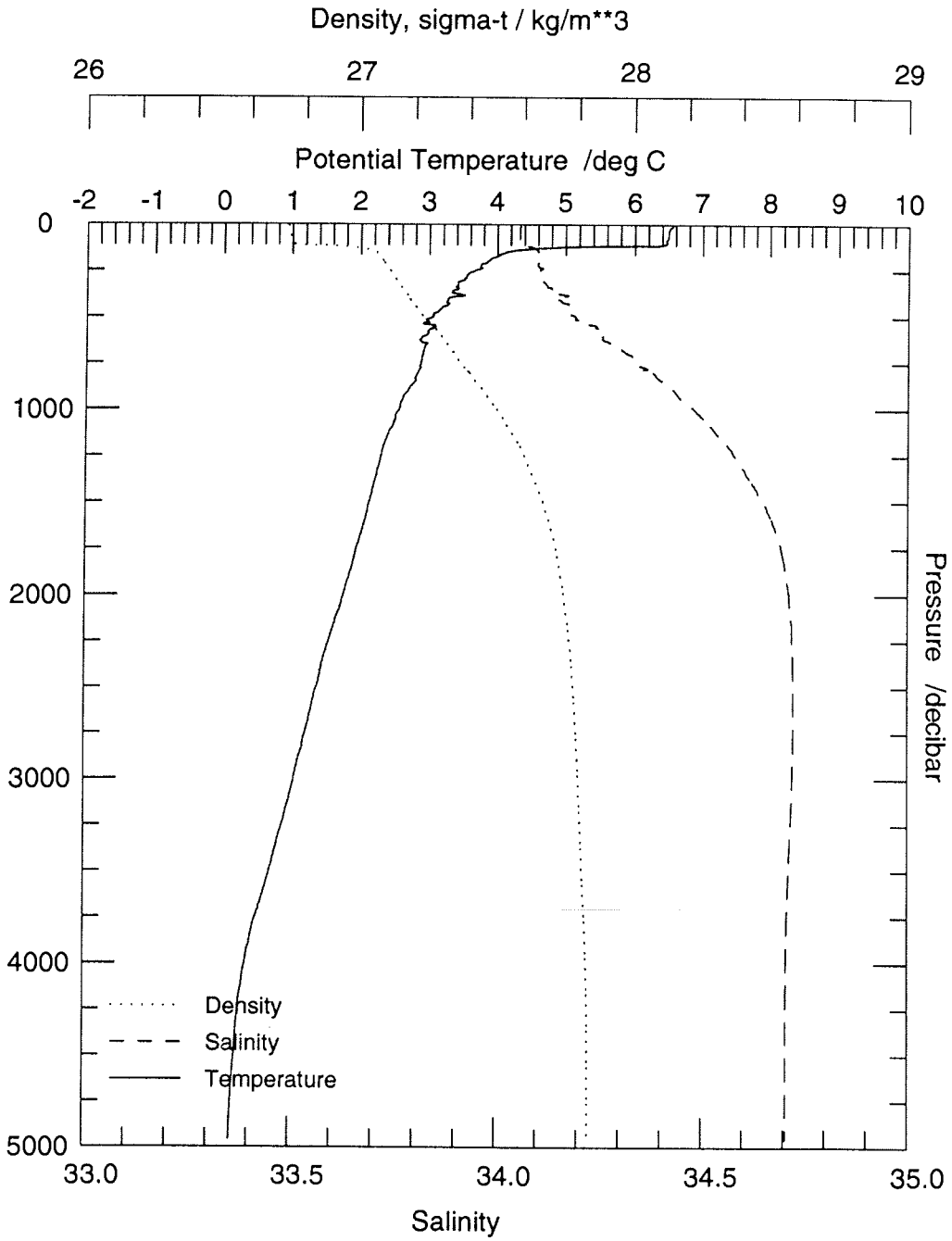

Station: 60 ANT XII/4 1995

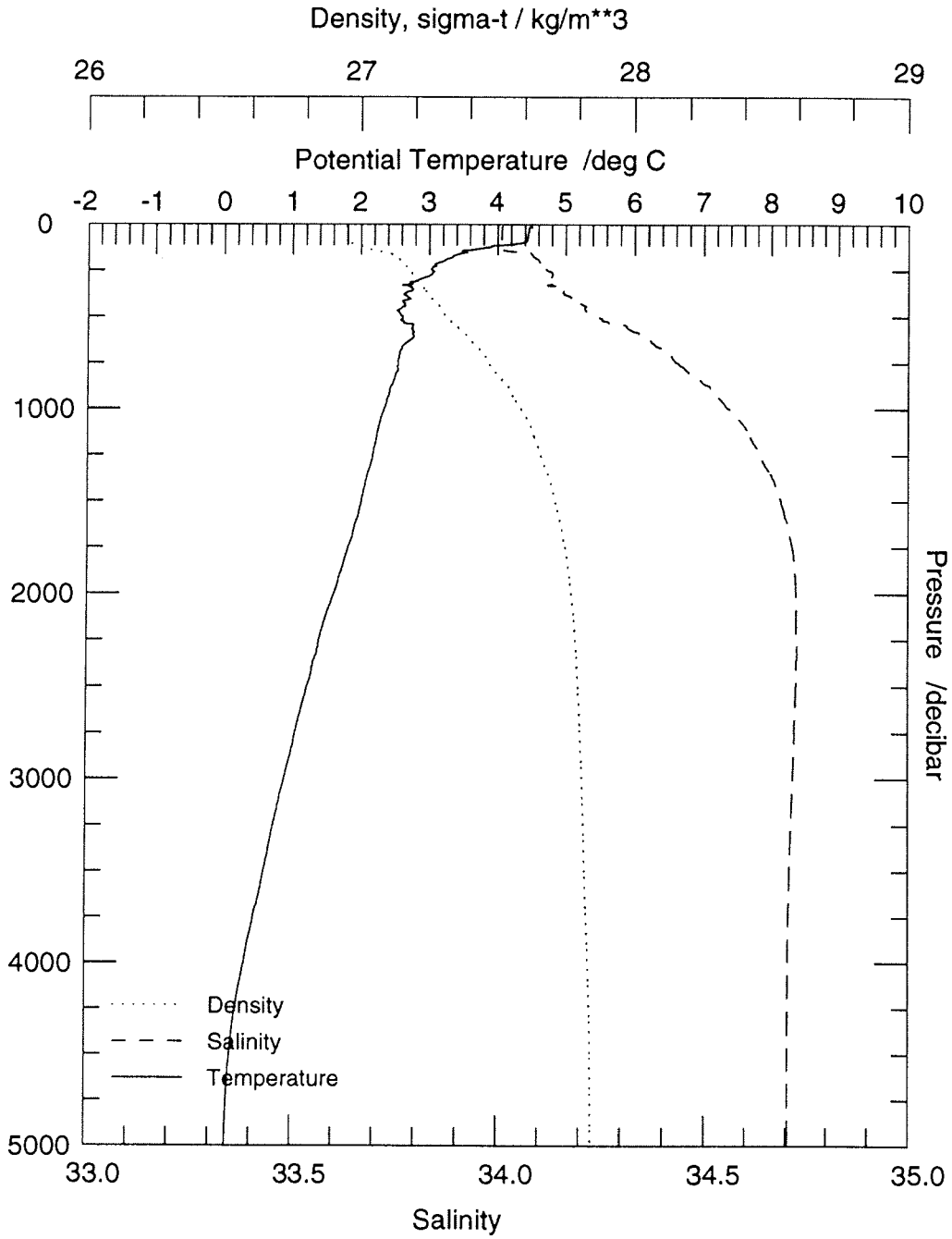

Station: 80 ANT XII/4 1995

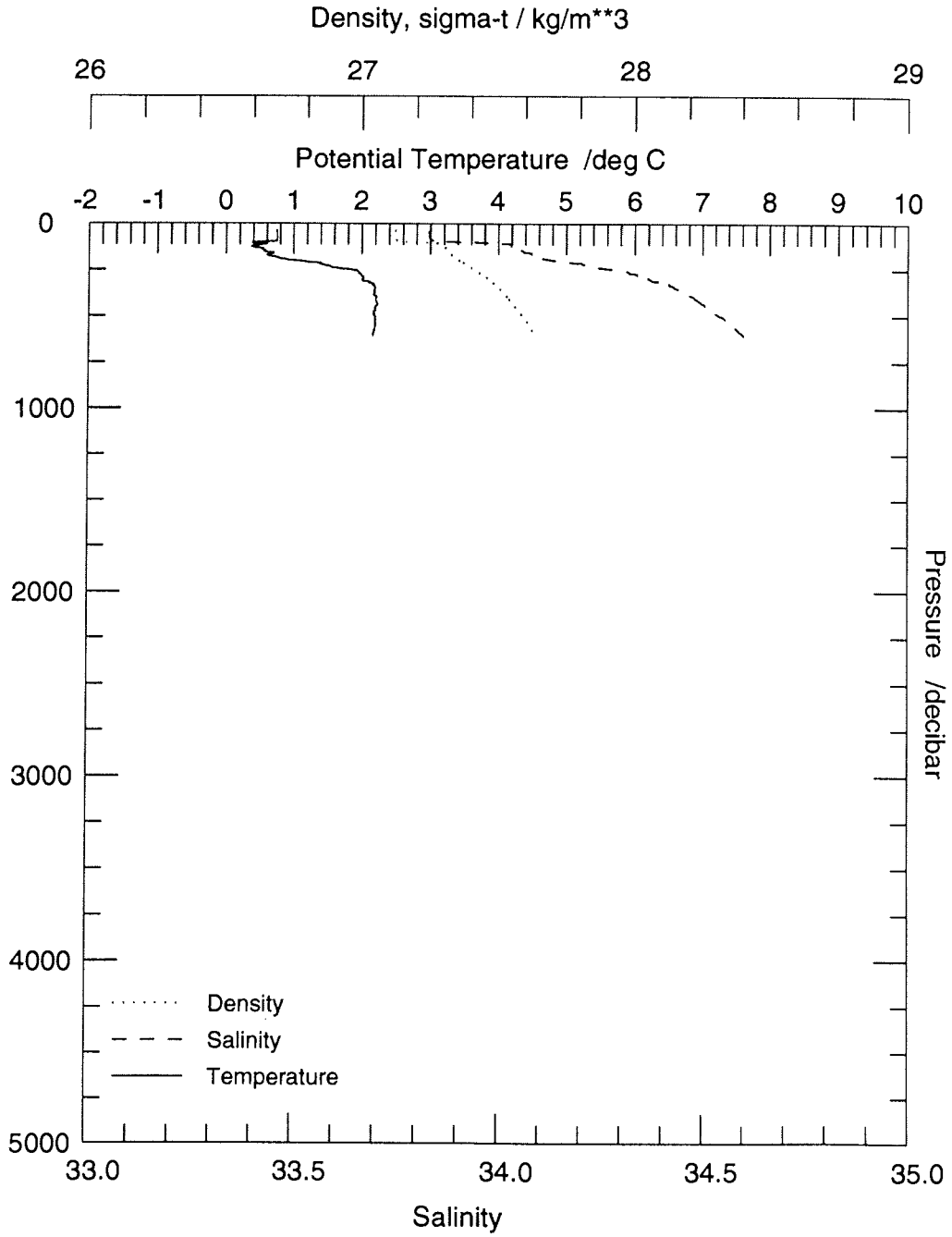

Station: 91 ANT XII/4 1995

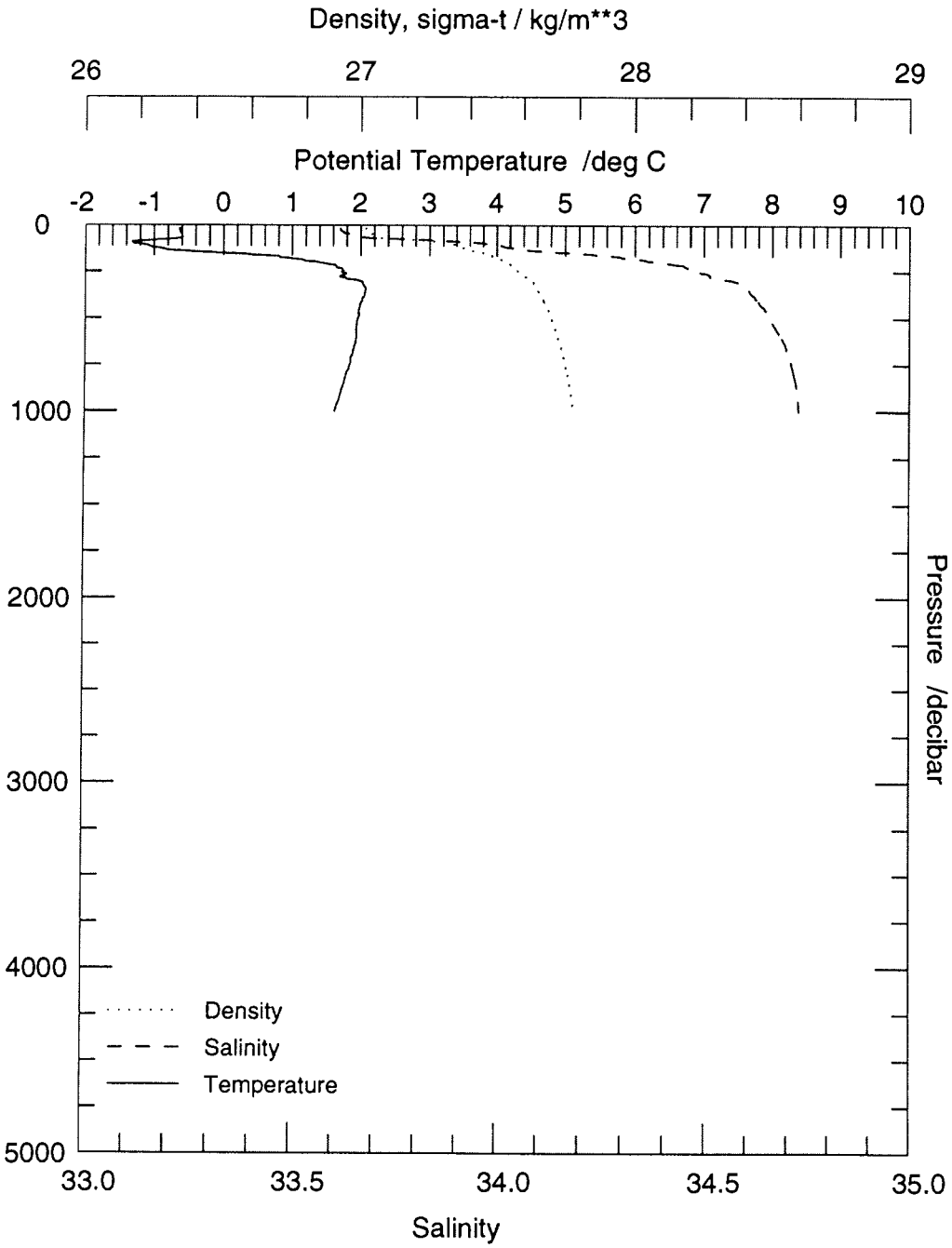

Station: 103 ANT XII/4 1995

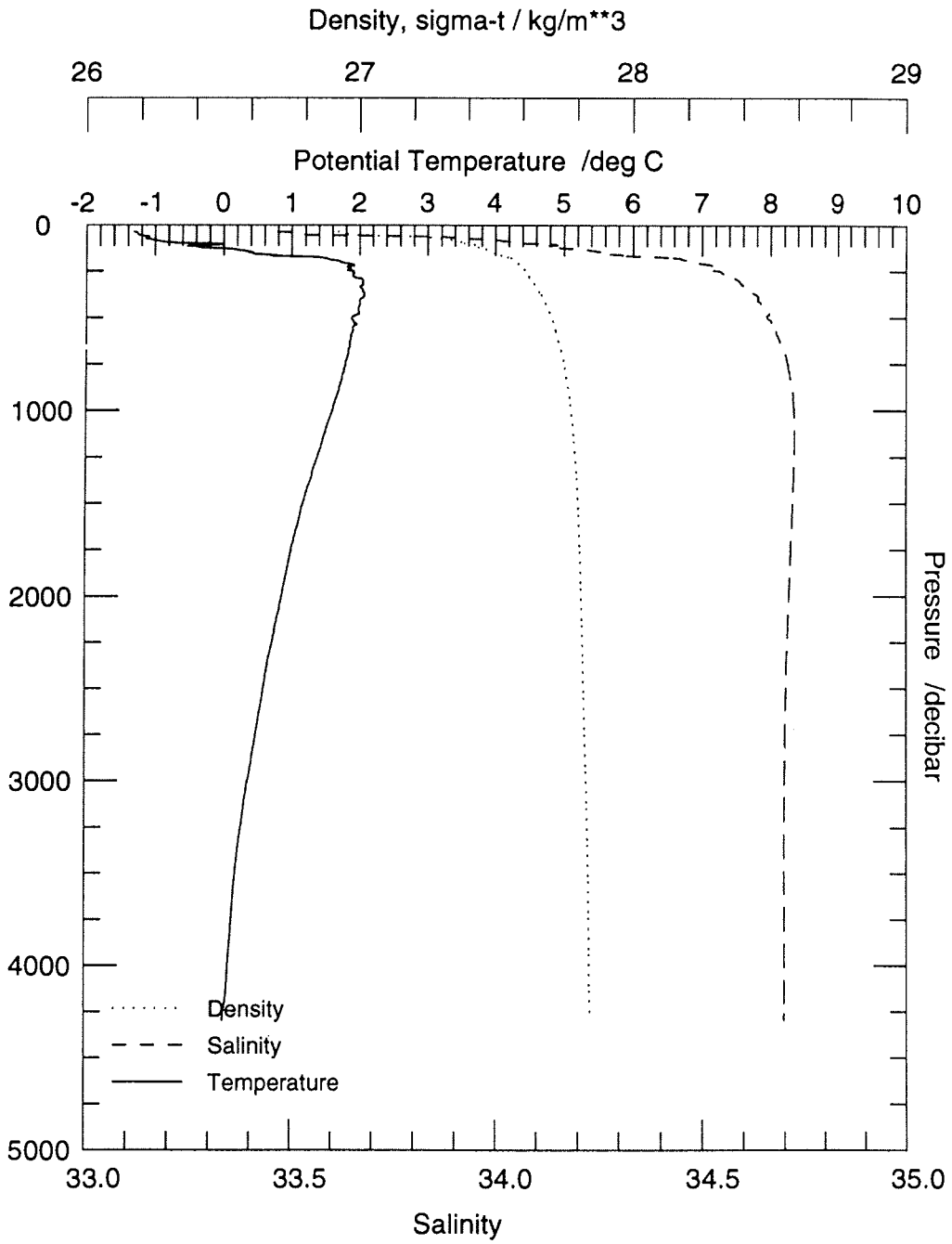

Station: 104 ANT XII/4 1995

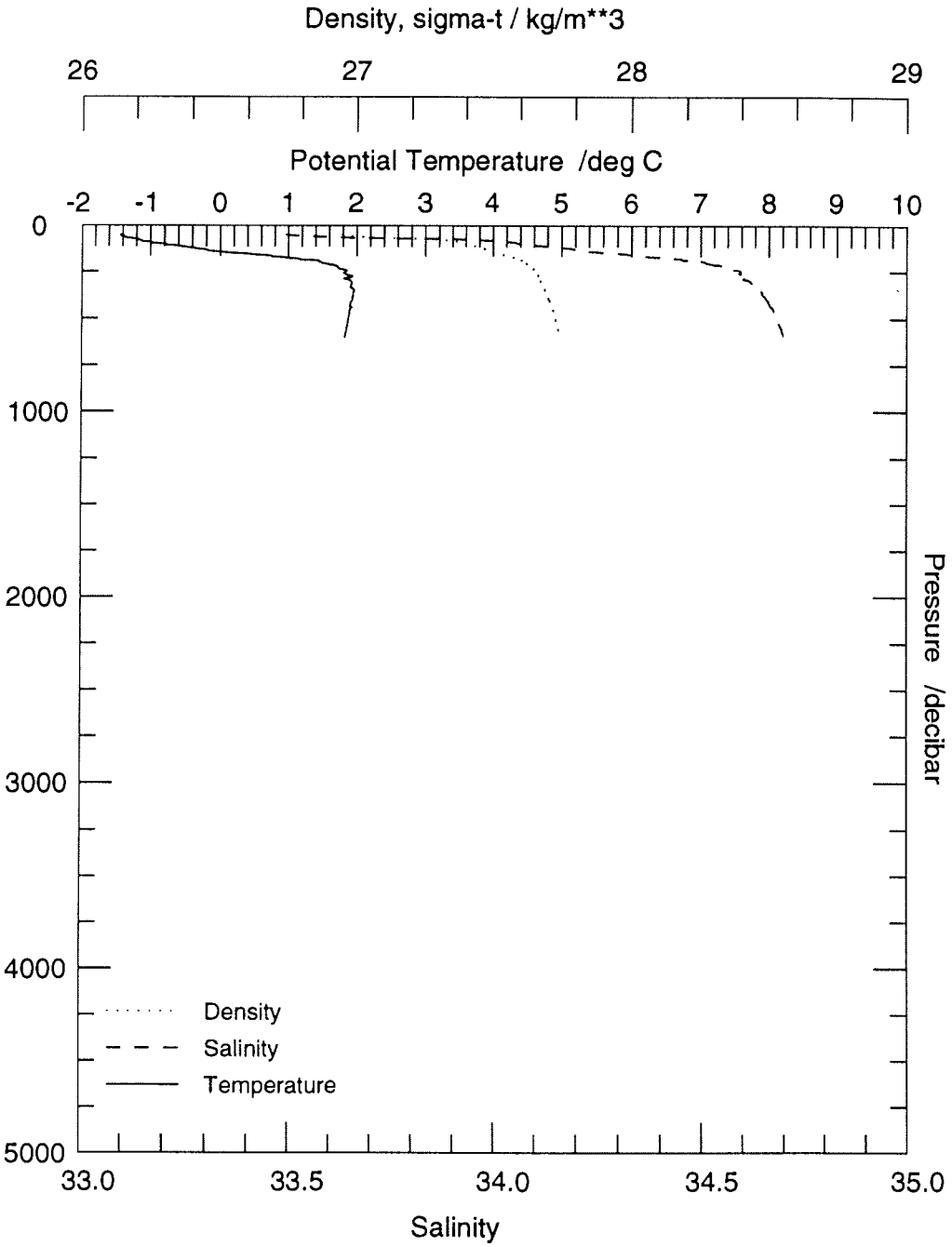

Station: 135 ANT XII/4 1995

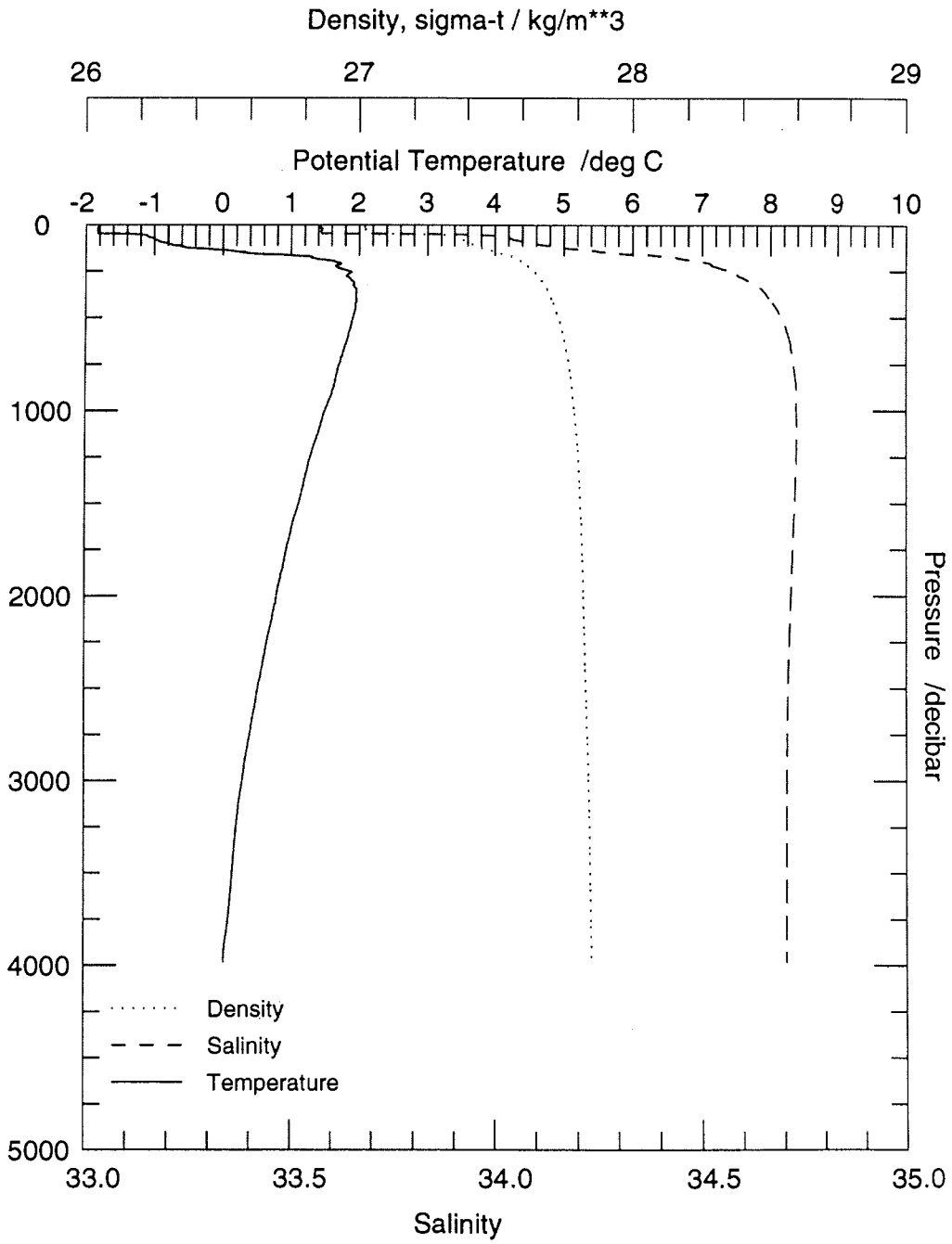

Station: 138 ANT XII/4 1995

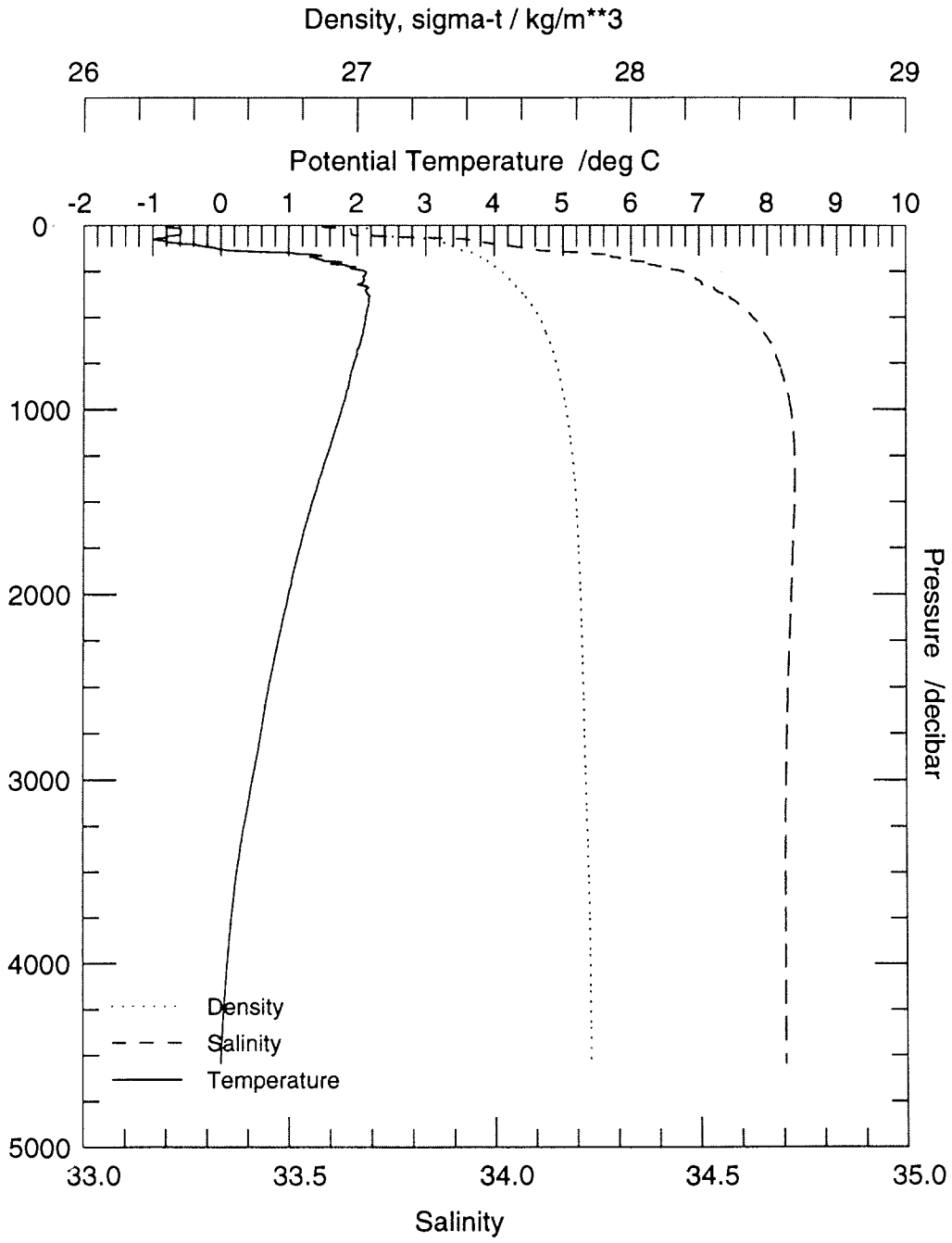

Station: 141 ANT XII/4 1995

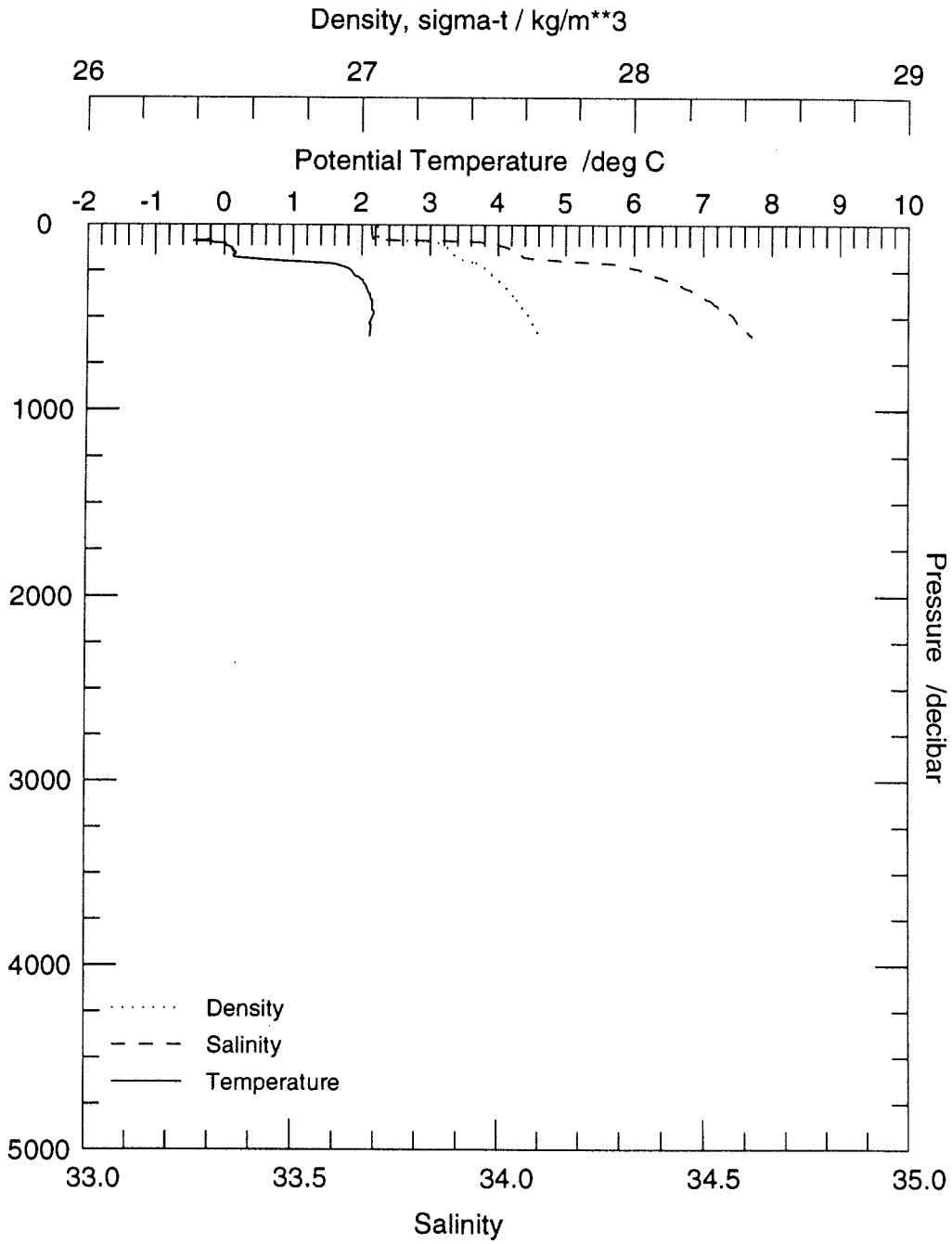

Station: 154 ANT XII/4 1995

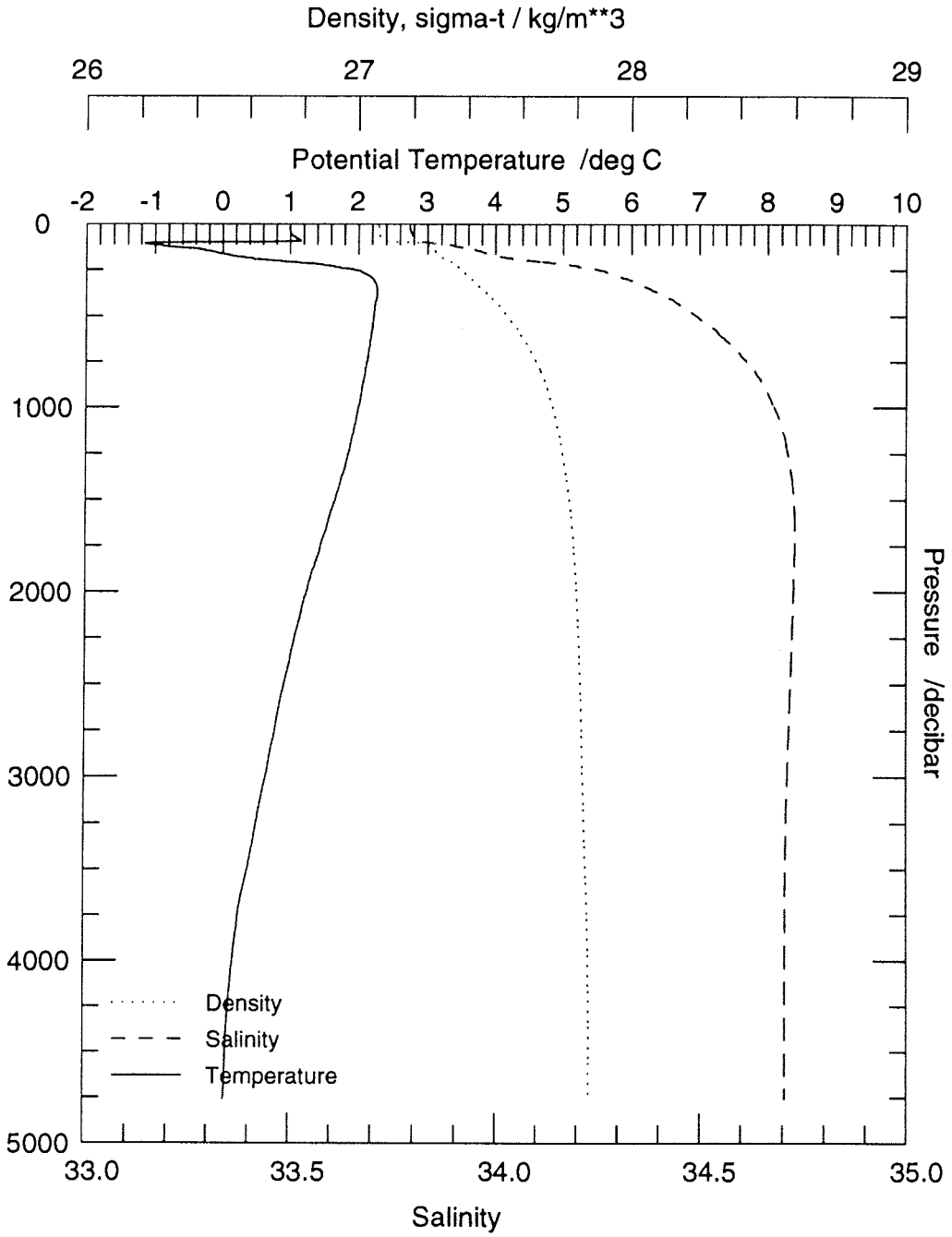

Station: 162 ANT XII/4 1995

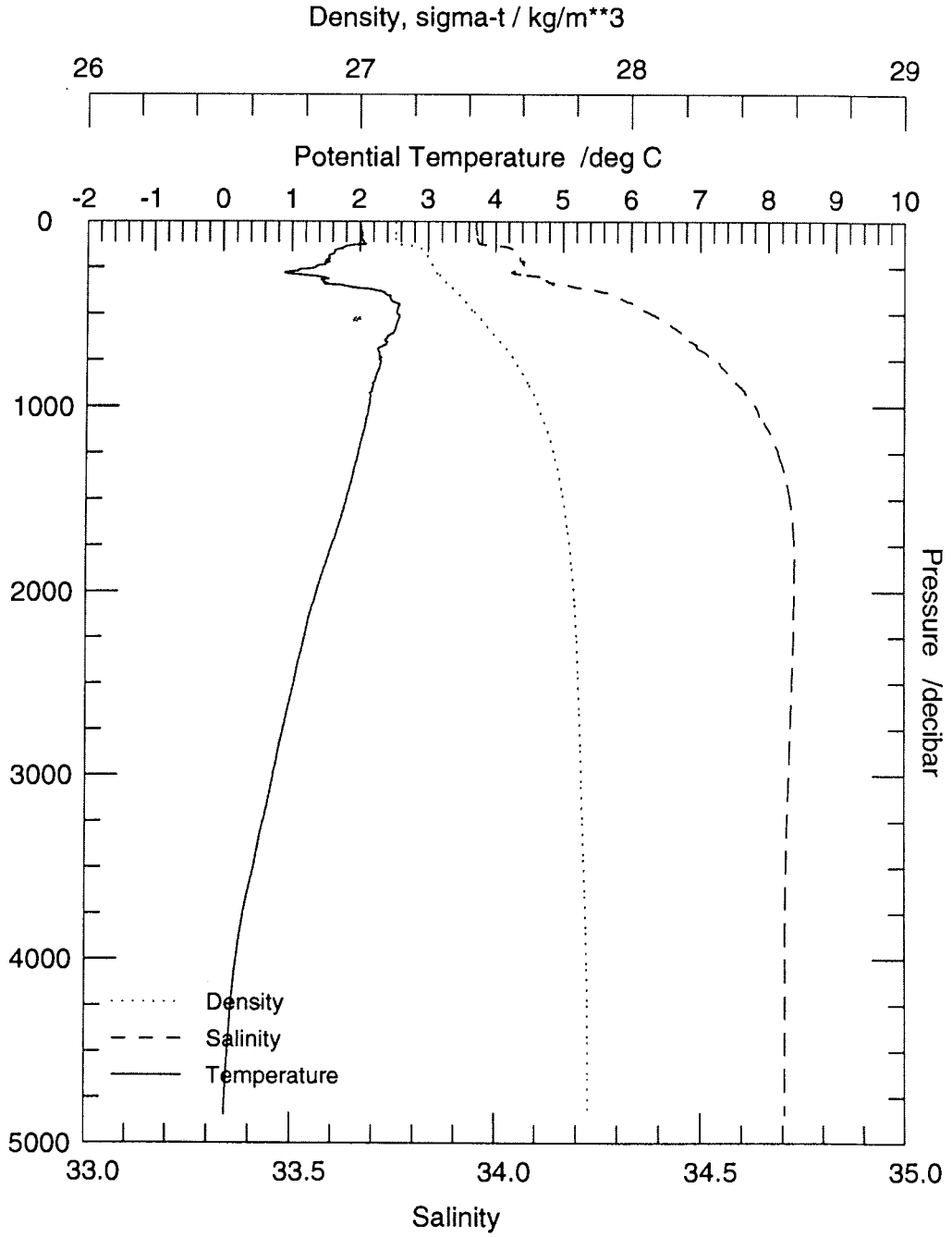

Station: 166 ANT XII/4 1995

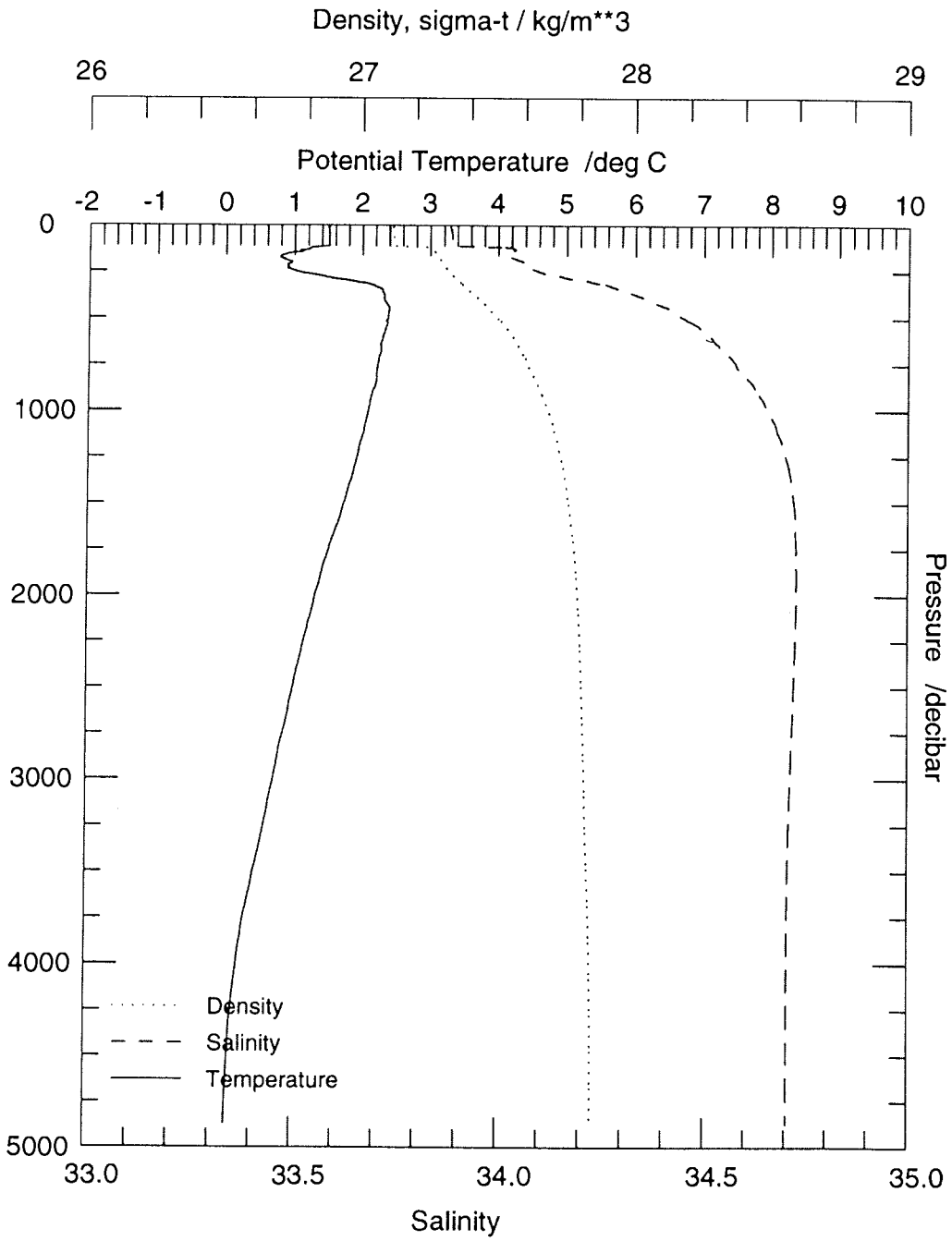

Station: 172 ANT XII/4 1995

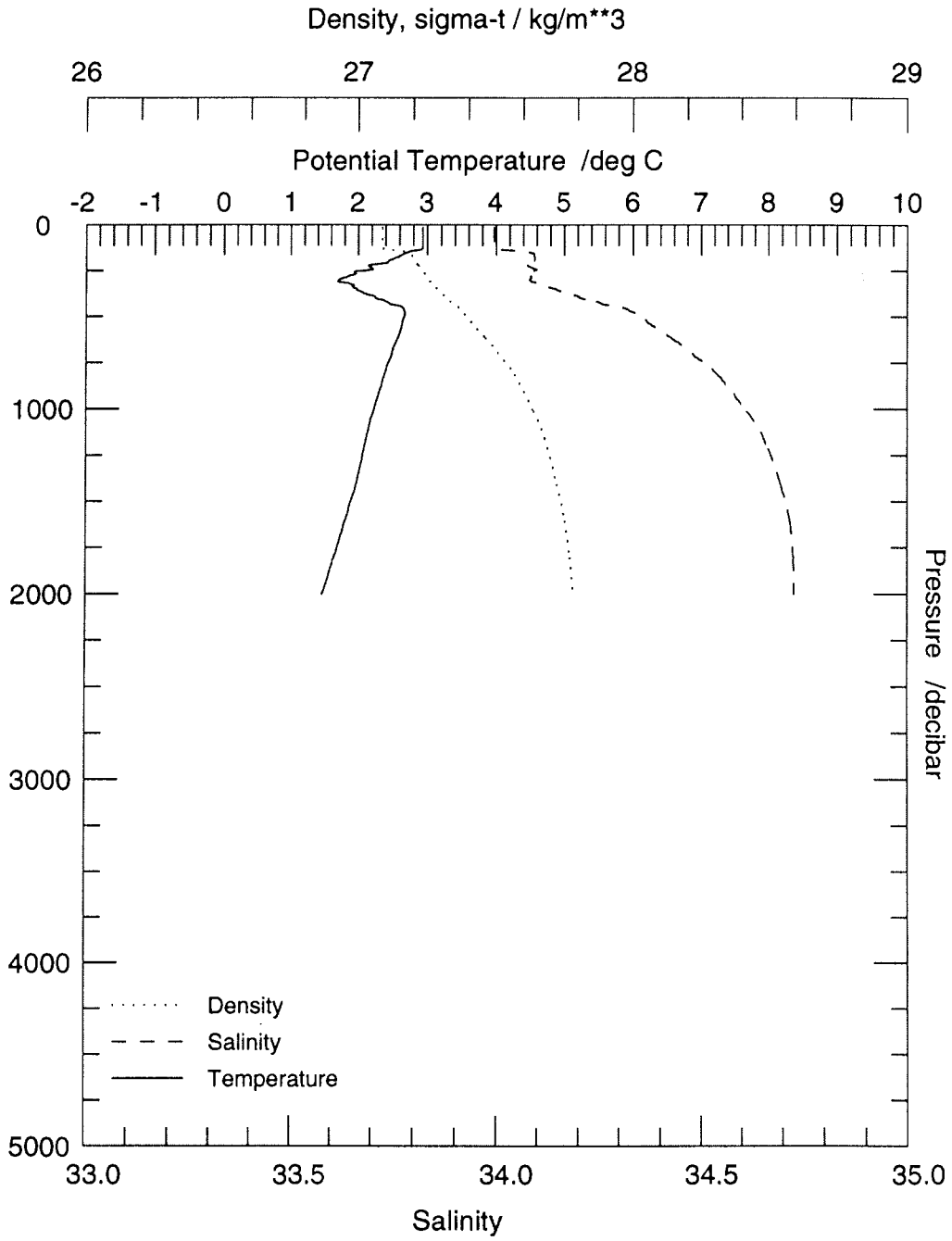

Station: 177 ANT XII/4 1995

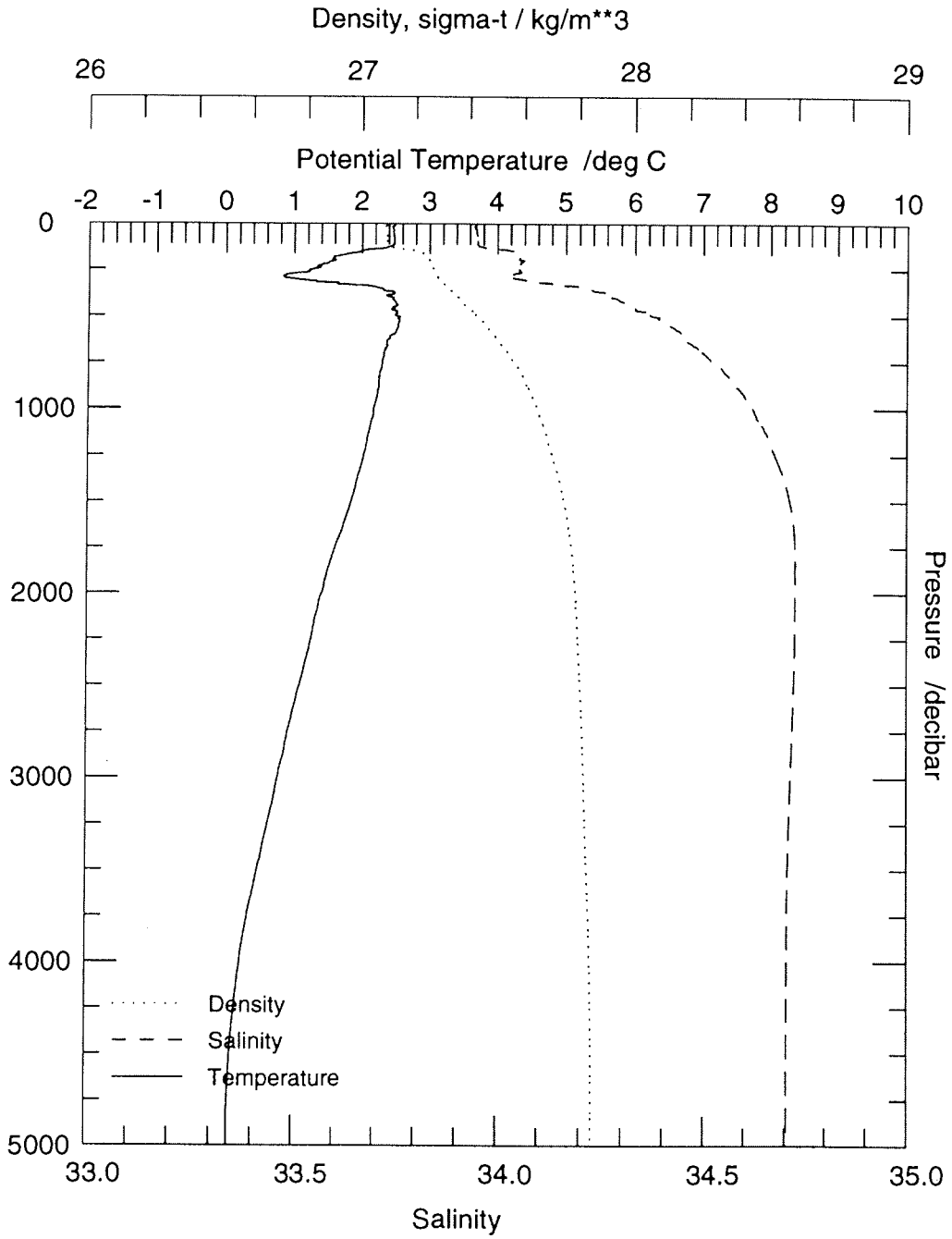

Station: 182 ANT XII/4 1995

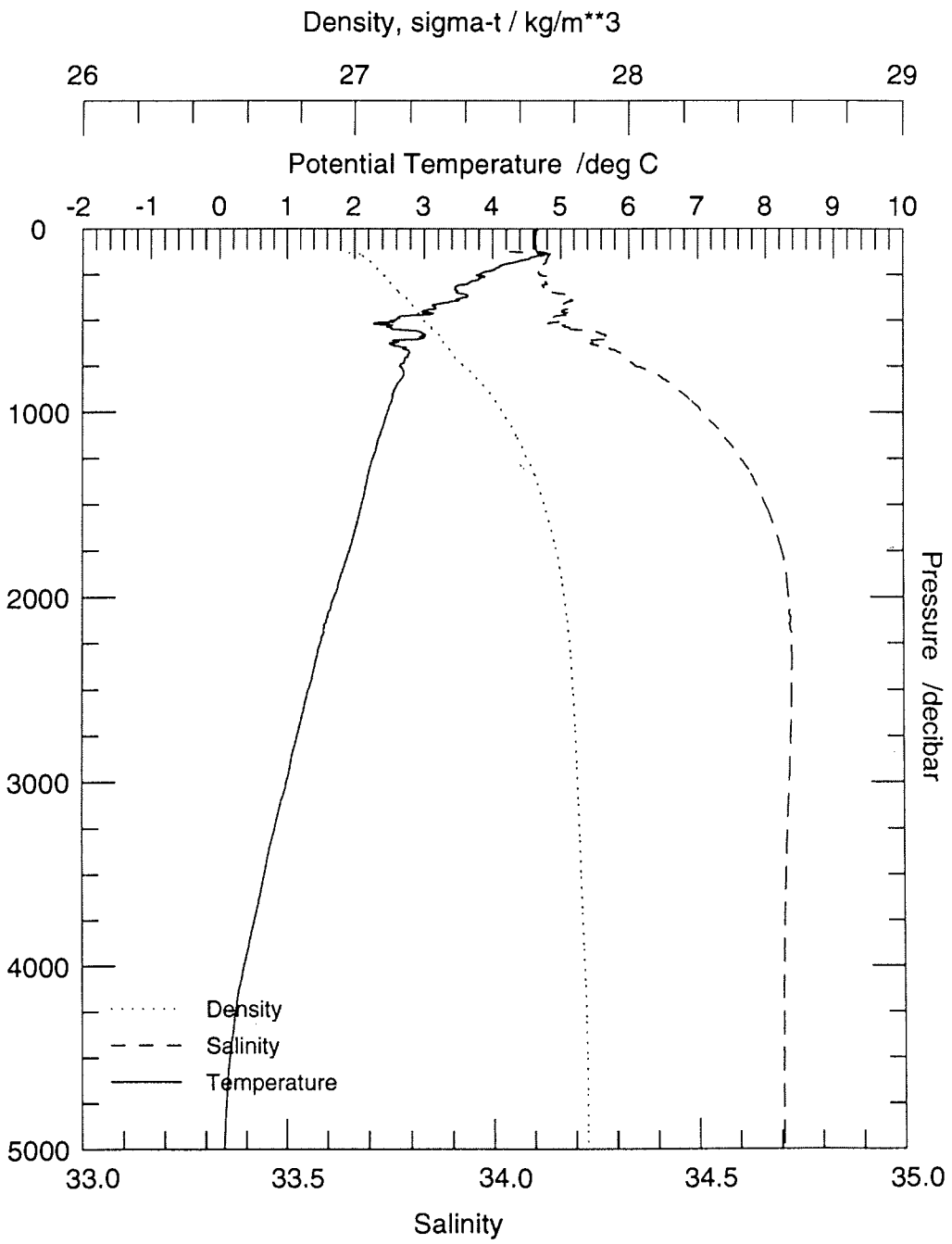

Station: 186 ANT XII/4 1995

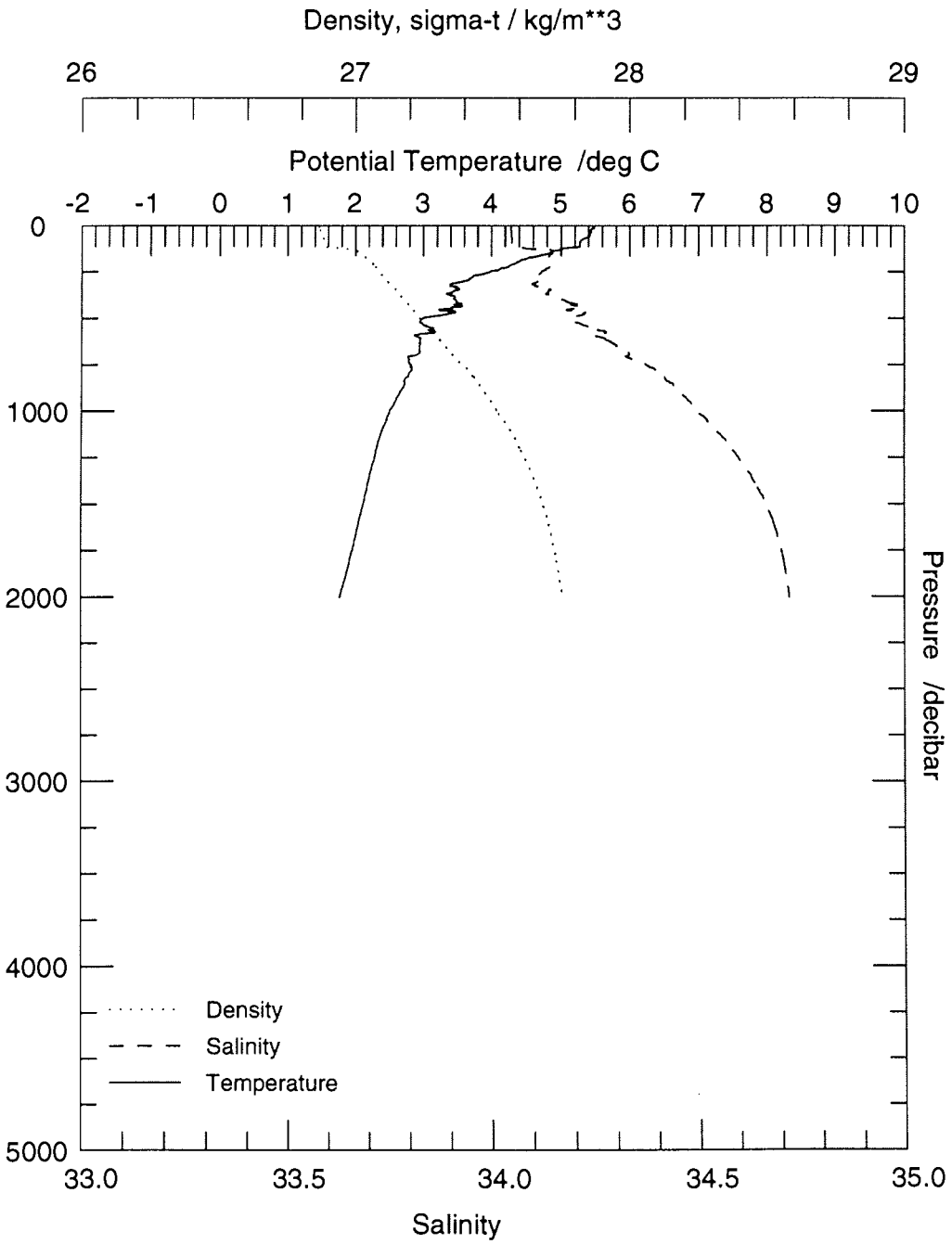

Station: 207 ANT XII/4 1995

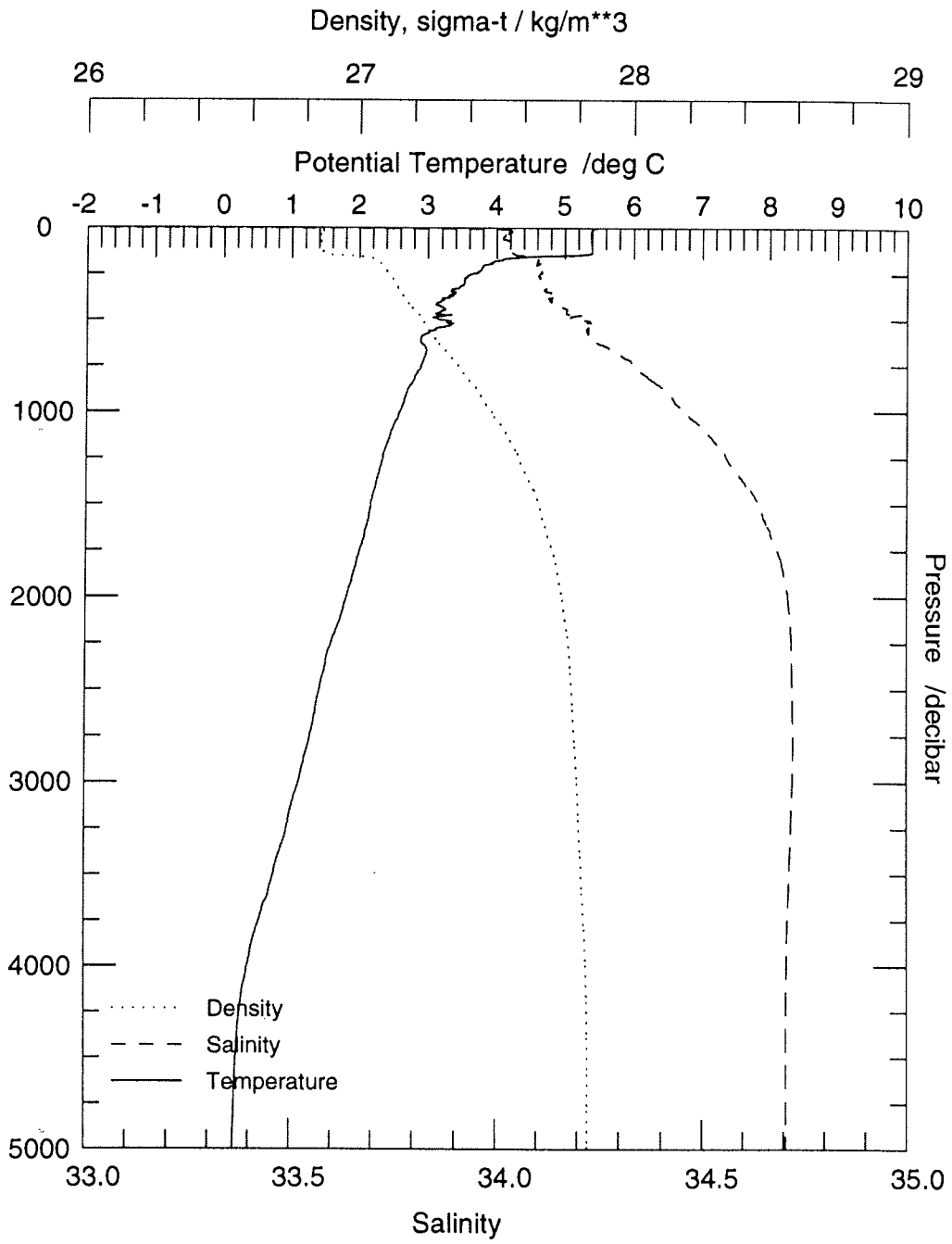

5 Sections

Presented sections show the distribution of the properties in the region of Antarctic Intermediate Water (stations 1-14 and 14-47) and across the Antarctic Circumpolar Current. Numbers of the stations are indicated on the top of the plots.

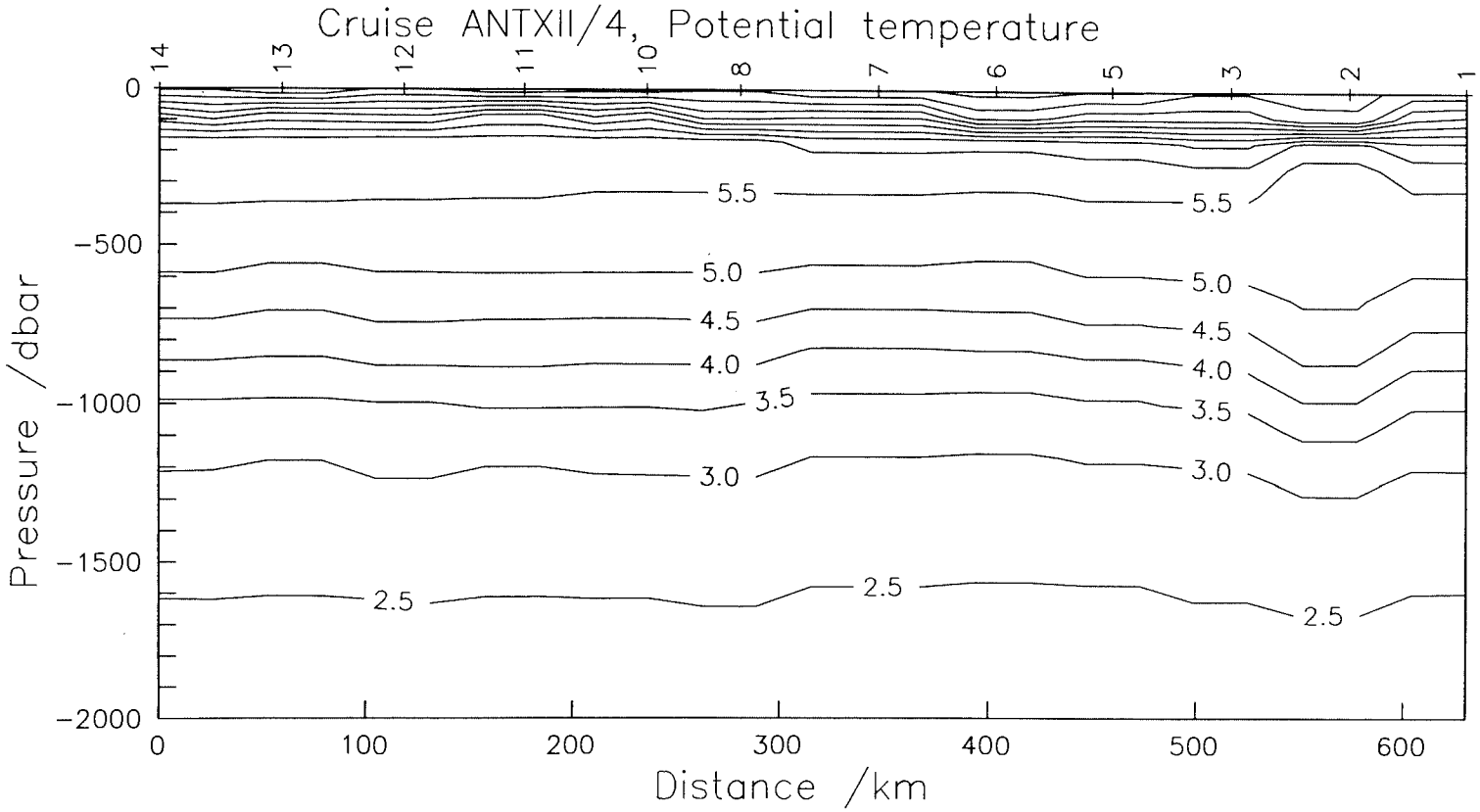
Cruise ANTXII/4, Potential temperature
14
13
12
11
10
8
7
6
5
3
2
1
0
-500
-1000
-1500
-2000
Pressure /dbar
5.5
5.0
4.5
4.0
3.5
3.0
2.5
0
100
200
300
400
500
600
Distance /km

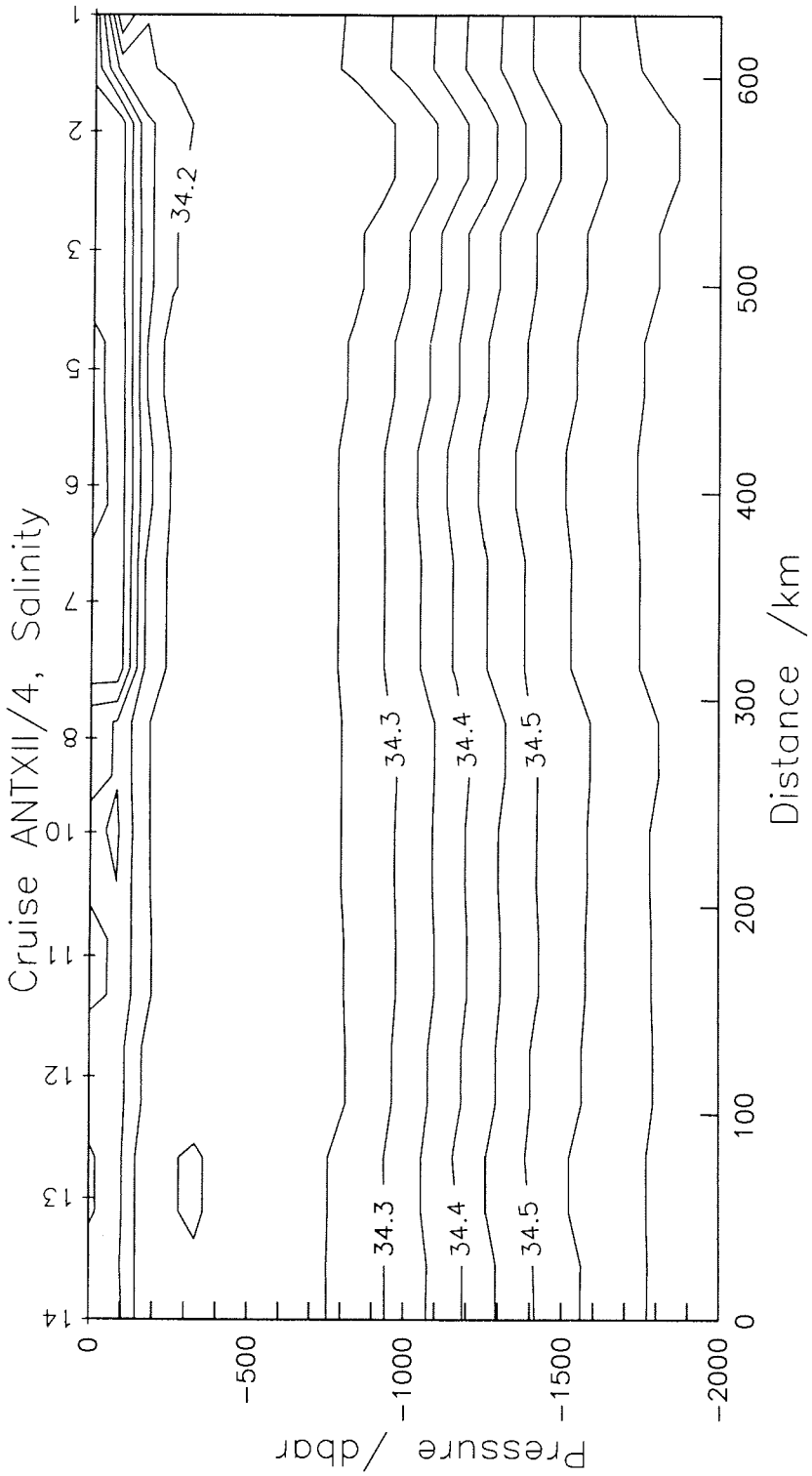
Cruise ANTXII/4, Salinity
Pressure /dbar
Distance /km
34.2
34.3
34.4
34.5
0
-500
-1000
-1500
-2000
100
200
300
400
500
600

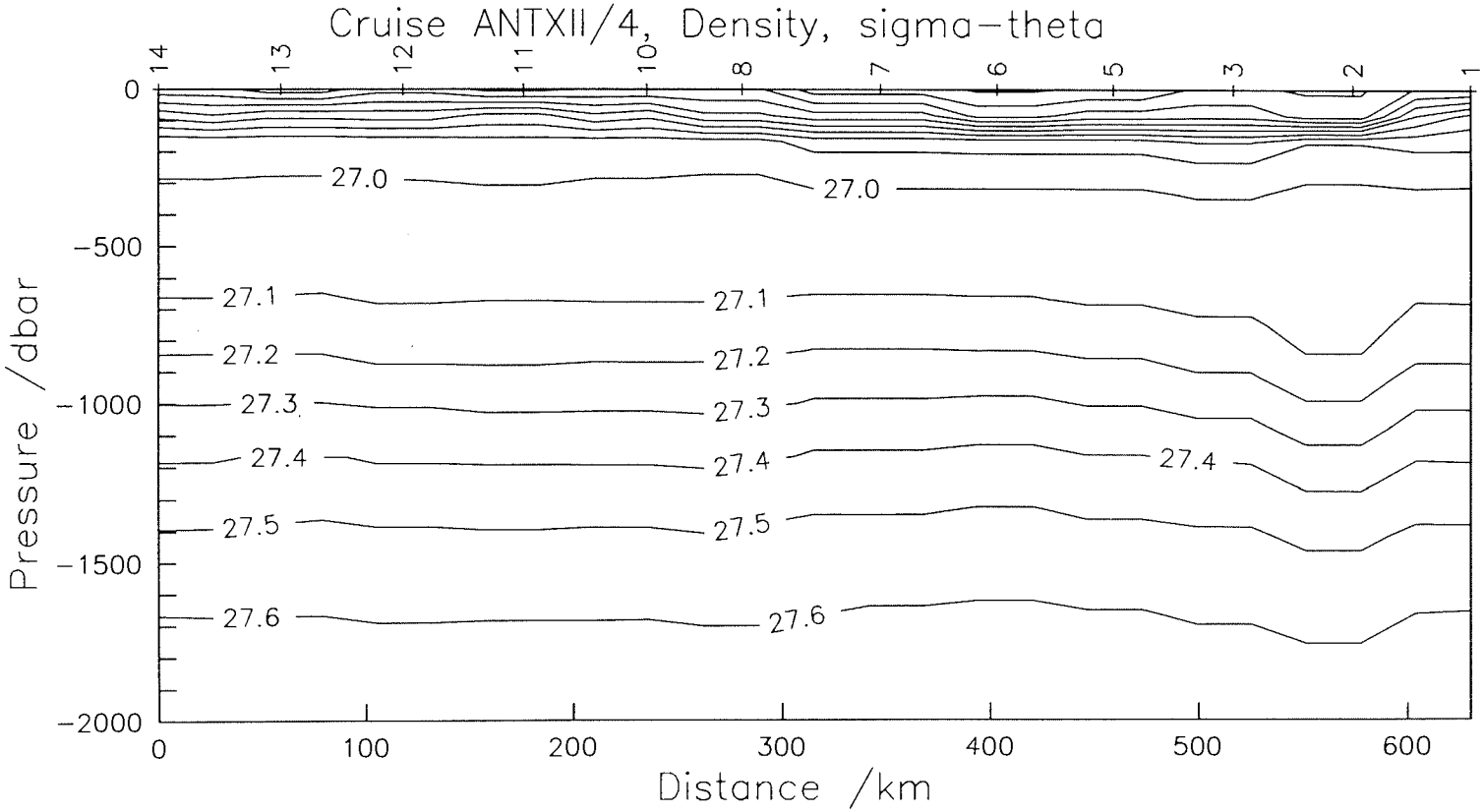
Cruise ANTXII/4, Density, sigma-theta
14
13
12
11
10
8
7
6
5
3
2
1
0
-500
-1000
-1500
-2000
Pressure /dbar
27.0
27.0
27.1
27.1
27.2
27.2
27.3
27.3
27.4
27.4
27.4
27.5
27.5
27.6
27.6
0
100
200
300
400
500
600
Distance /km

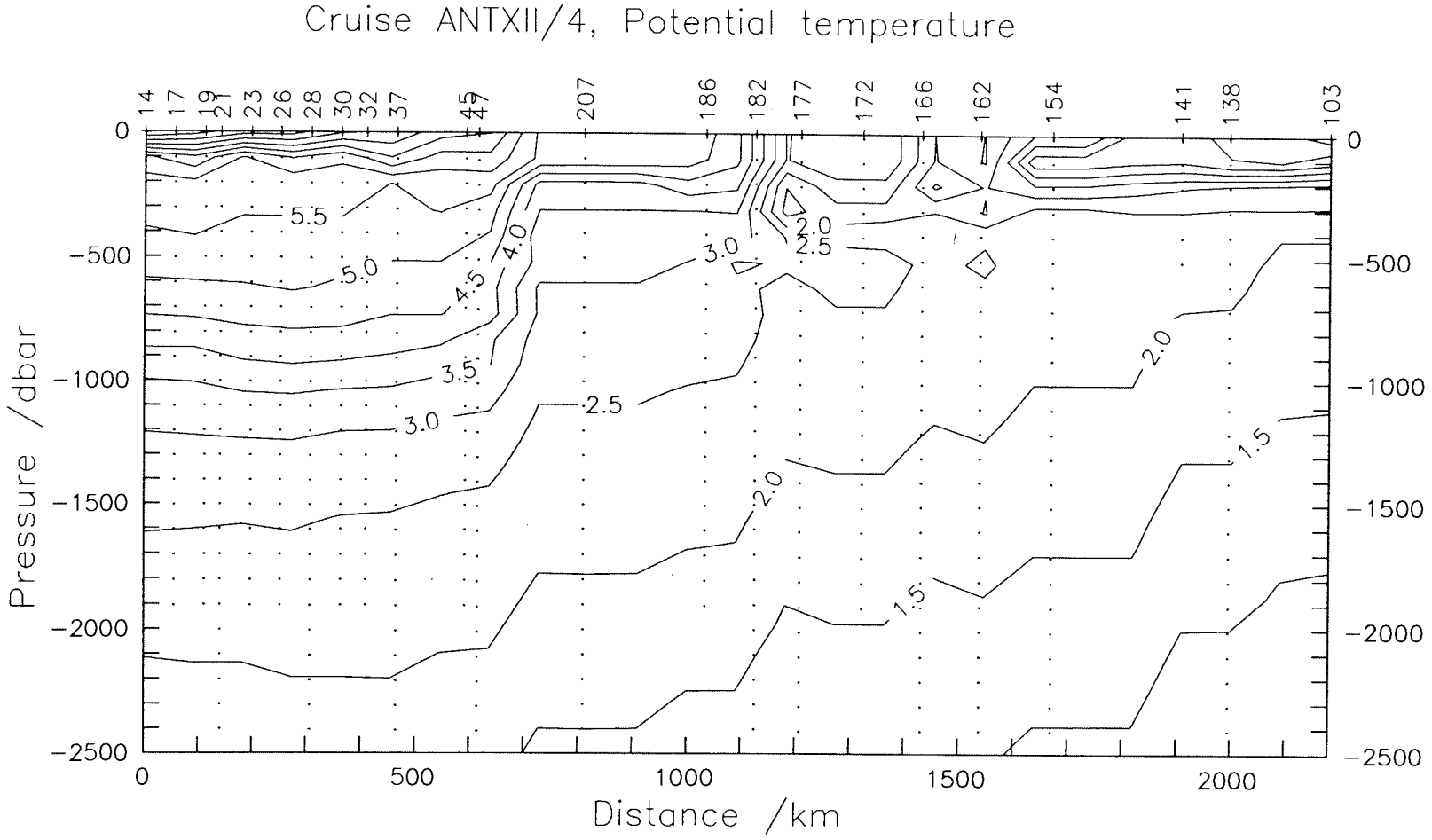
Cruise ANTXII/4, Potential temperature
14 17 19 21 23 26 28 30 32 37 45 47 207 186 182 177 172 166 162 154 141 138 103
0
-500
-1000
-1500
-2000
-2500
5.5
5.0
4.5
4.0
3.5
3.0
2.5
2.0
1.5
Pressure /dbar
0
500
1000
1500
2000
Distance /km

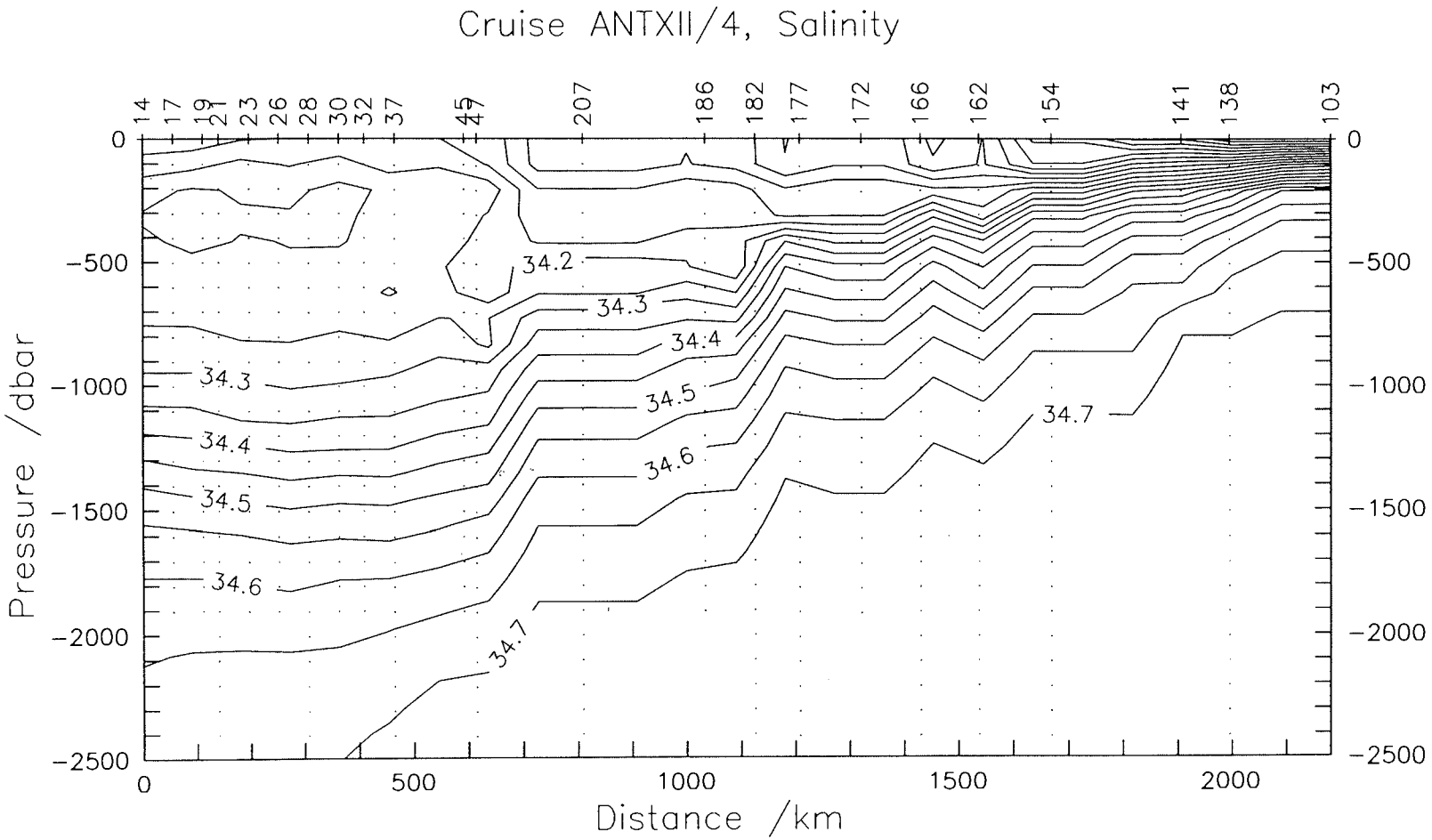
Cruise ANTXII/4, Salinity
14 17 19 21 23 26 28 30 32 37 45 47 207 186 182 177 172 166 162 154 141 138 103
0
-500
-1000
-1500
-2000
-2500
34.2
34.3
34.4
34.5
34.6
34.7
Pressure /dbar
0
500
1000
1500
2000
Distance /km

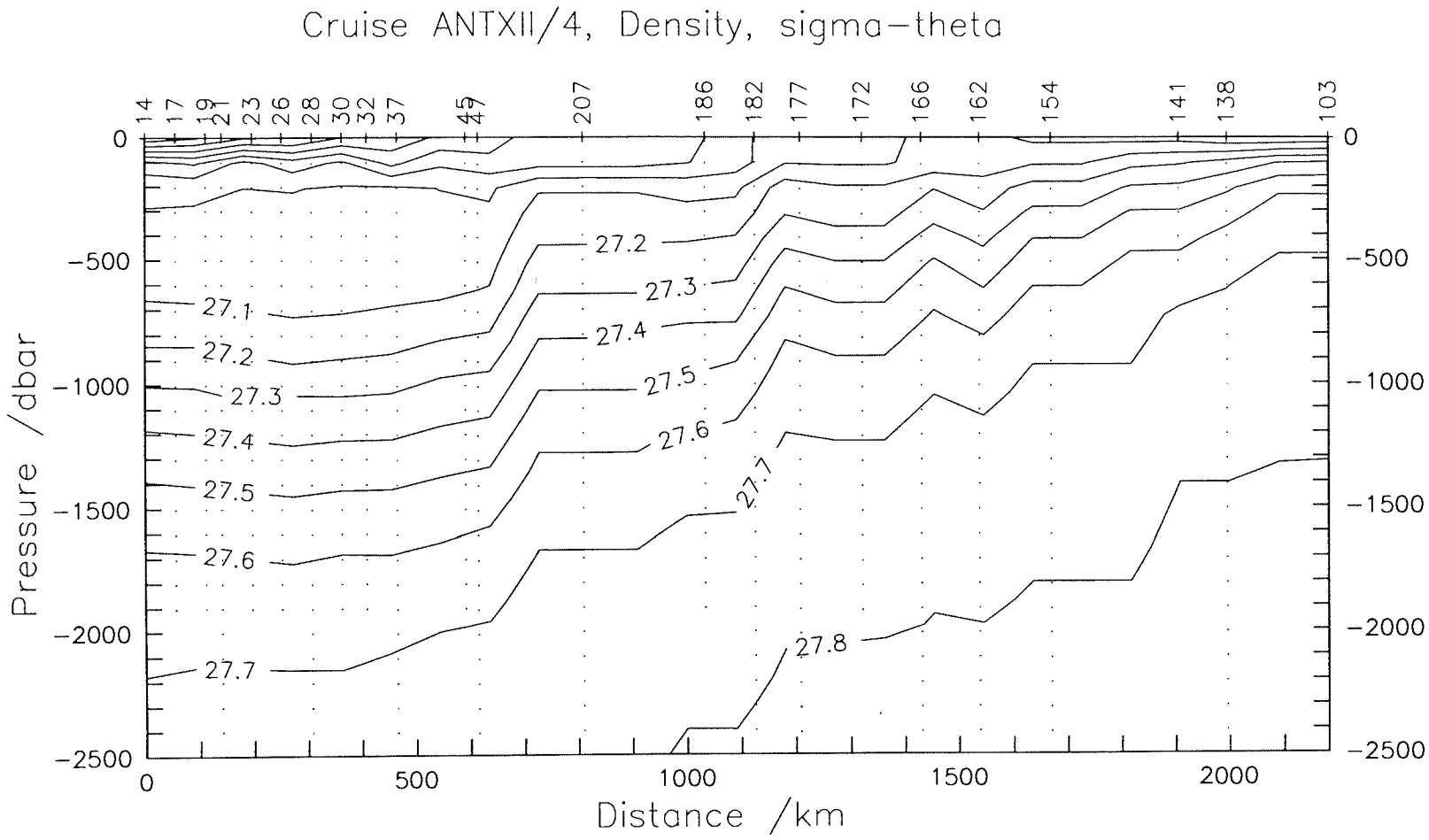
Cruise ANTXII/4, Density, sigma-theta
14 17 19 21 23 26 28 30 32 37 45 47 207 186 182 177 172 166 162 154 141 138 103
0
-500
-1000
-1500
-2000
-2500
Pressure /dbar
27.1
27.2
27.3
27.4
27.5
27.6
27.7
27.8
0
500
1000
1500
2000
Distance /km

Similarity of non dimensional density profiles.

Qualitative inspection of potential density distribution (σ_Θ) reveals notable similarity in the vertical profiles that can be recognised if one follows three adjacent density isolines in an increasing order (for example 27.5, 27.6 and 27.7 $kg \cdot m^{-3}$ numbered as isolines 1, 2 and 3 respectively; see page 55). It can be seen that the vertical distance of the isoline 2 relative to the isolines 1 and 3 remains constant over a long spatial distance whereas the absolute vertical layer thickness confined between these isolines changes considerably. Otherway stated, it means that any density difference in the considered layer, normalised by the maximum density difference of the layer, is a function of the non dimensional vertical co-ordinate:

$$\frac{\sigma_\Theta^1 - \sigma_\Theta}{\sigma_\Theta^1 - \sigma_\Theta^3} = f(p_n)$$

Here the superscript stands for an isoline number, $p_n = \frac{p^1 - p}{p^1 - p^3}$ is a non dimensional vertical co-ordinate and p - a pressure level of the corresponding isopycnal. Figure 2 shows the vertical profiles of non dimensional density, calculated for the layer confined between the isopycnals 27.5 and 27.7 kgm^{-3}. It can be seen that similarity is characteristic to an area about 1500 km wide which locates in the region of water mass transformation from Sub Antarctic- to Antarctic waters.

Physical reasons, responsible for the observed similarity are not evident.

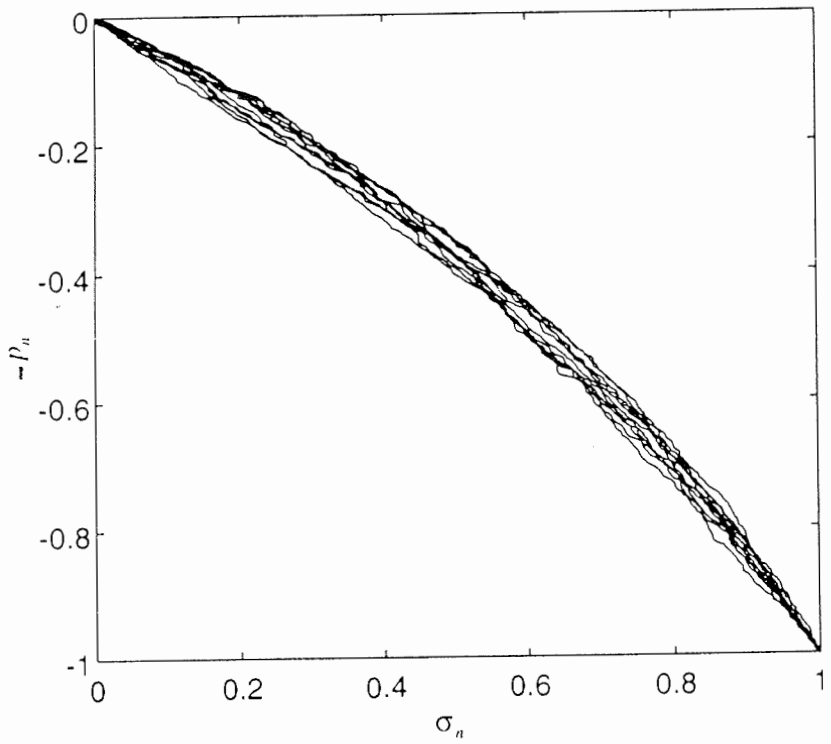

Figure 2. Non dimensional density profiles $\sigma_n = \left(\sigma_\Theta^1 - \sigma_\Theta\right) / \left(\sigma_\Theta^1 - \sigma_\Theta^2\right)$ (where $\sigma_\Theta^1 = 27.5\, kgm^{-3}$, $\sigma_\Theta^2 = 27.7\, kgm^{-3}$, $\sigma_\Theta^1 \le \sigma_\Theta \le \sigma_\Theta^2$) as a function of non dimensional layer thickness $p_n = \left(p^1 - p\right) / \left(p^1 - p^2\right)$ calculated for the deep stations: 14, 21, 28, 37, 47, 55, 60, 162, 166, 177, 182.

Following simple arguments show that similarity can be regarded as a limiting case of stationary mixing along neutral surfaces in the continuously stratified ocean with a constant horizontal pressure gradient which is balanced by the Coriolis force (i.e. one has constantly sloping isopycnals as it is the case in the region of the Antarctic Circumpolar Current). In this limiting case, temperature and salinity gradients along isopycnic surfaces are zero. It appears then also that all vertical temperature and salinity profiles coincide in a potential temperature - salinity diagram and hence the surfaces of potential densities referenced to different reference pressures and neutral surfaces coincide with each other in the *x, y, z* space. Figure 3 gives such example and demonstrates that in the region of the Antarctic Circumpolar Current potential density surfaces, referenced to zero and 2000 dbar level, are to a good approximation parallel. The other way to state the same argument is to use the definition of the neutral surfaces (*McDougall* 1987)

$$\frac{1}{\rho}\nabla_n \rho = \gamma \nabla_n p, \qquad (1)$$

where $\nabla_n = \left.\frac{\partial}{\partial x}\right|_n i + \left.\frac{\partial}{\partial y}\right|_n j$ is a neutral surface gradient operator, *x* and *y* are horizontal co-ordinates and *i* and *j* are unit vectors in these directions and $\gamma = \left(\frac{1}{\rho}\frac{\partial \rho}{\partial p}\right)_{\theta,S}$ is a coefficient of adiabatic and isentropic compressibility (subscripts mean that potential temperature and salinity being kept constant). (1) multiplied by a characteristic distance L, can be rewritten in the form of finite differences:

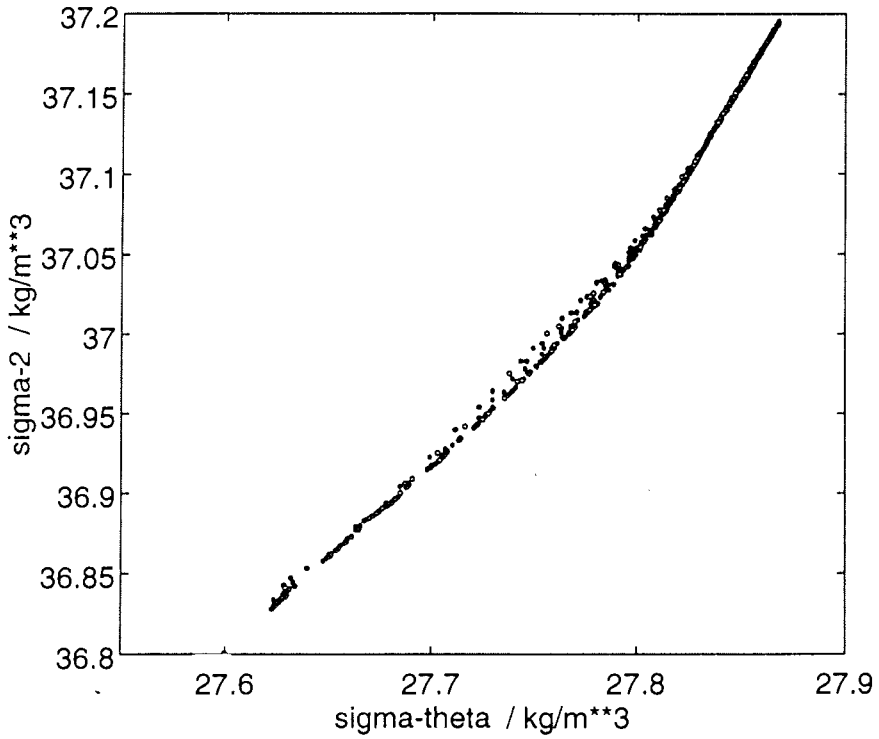

Figure 3. $\sigma_2 - \sigma_\Theta$ diagram. Shows that the isolines of potential density surfaces referenced to different pressure levels are in *x, y, z* space to a good approximation parallel. Calculated for the stations: 14, 17, 19, 21, 23, 26, 28, 30, 32, 37, 45, 47, 55, 60, 138, 141, 154, 162, 166, 172, 177, 182, 186, 207.

$$\sigma_r = \rho - \rho\gamma(p - p_r), \qquad (2)$$

where $\sigma_r = \sigma(\theta, S, p_r)$ is a particles' density referenced to a pressure level p_r and $\rho = \rho(\theta, S, p)$ - *in situ* density. (2) expresses the fact that the local tangent plane of an isopycnic surface coincides with the tangent plane of a neutral surface (McDougall, 1984). Fixing any of the reference pressure levels while moving in the direction of increasing or decreasing pressure means that (2) can be used for the calculation of a potential density surface that in general case do not coincide with a neutral surface. Noting now that potential density, referenced to zero pressure can be expressed as $\sigma_\Theta = \rho - \rho_c \gamma p$ (where ρ_c is a constant), (2) can be rewritten in the form:

$$\sigma_r - \sigma_\Theta = -\rho_c \gamma p_r \qquad (3)$$

For a water particle that moves adiabatically and isentropically in the ocean, (3) is constant for a fixed pressure reference level or changes proportionally to the latter if the reference pressure is changing. For a couple of water particles:

$$\left(\sigma_r^2 - \sigma_r^1\right) - \left(\sigma_\Theta^2 - \sigma_\Theta^1\right) = \rho_c\left(\gamma^2 - \gamma^1\right)p_r \qquad (4)$$

Now making use of non linearity in the equation of state $\partial^2\rho/\partial p \partial\Theta$ and $\partial^2\rho/\partial p \partial S$, the finite difference for adiabatic and isentropic compressibility for any pair of water particles can be expressed as following:

$$\gamma_2 - \gamma_1 = -\frac{\partial\alpha}{\partial p}d\Theta + \frac{\partial\beta}{\partial p}dS \qquad (5)$$

where $\alpha = -1/\rho(\partial\rho/\partial\Theta)_{S,p}$ and $\beta = 1/\rho(\partial\rho/\partial S)_{\Theta,p}$ are the thermal expansion coefficient and saline contraction coefficient.

If the isopycnals of the potential density surfaces are parallel in *x,y,z* space then (4) remains constant for any fixed pressure reference level. Figure 4 which shows the dependence of $\rho_c(-\Delta\alpha\Delta\Theta + \Delta\beta\Delta S)$ on a layer thickness Δp, confirms that in the case of the considered hydrographic section the right side of (4) combined with (5) is to a good approximation constant for any fixed pair of potential density surfaces. The shape of the curve is determined by vertical temperature - salinity stratification (for the respective $\Theta - S$ diagram see Figure 5) and by the upper isopycnal chosen.

Finally, similarity of vertical non dimensional density profiles considered at the beginning of the paragraph, follows also from (4) and (5) if written in the normalised form:

$$\frac{(\sigma_r^1 - \sigma_r) - (\sigma_\Theta^1 - \sigma_\Theta)}{(\sigma_r^1 - \sigma_r^2) - (\sigma_\Theta^1 - \sigma_\Theta^2)} = \frac{(\gamma^1 - \gamma)}{(\gamma^1 - \gamma^2)} = f(p_n) \quad (6)$$

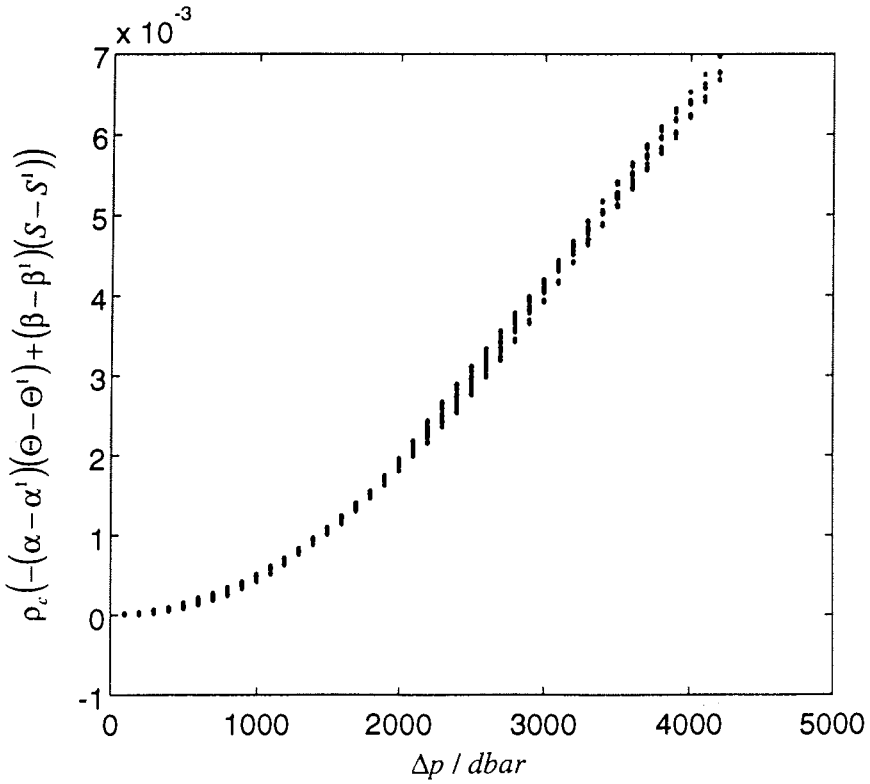

Figure 4. $c = \rho_c\left(-(\alpha-\alpha^1)(\Theta-\Theta^1)+(\beta-\beta^1)(S-S^1)\right)$ as a function of the layer thickness $\Delta p = (p-p^1)$, where p^1, Θ^1, S^1 are the values of pressure, potential temperature and salinity on the isopycnal $\sigma_2^1 = 36.8\ kgm^{-3}$ and p, Θ, S are the respective values for $\sigma_2 > \sigma_2^1$. Calculated for the stations: 14, 17, 19, 21, 23, 26, 28, 30, 32, 37, 45, 47, 55, 60, 138, 141, 154, 162, 166, 172, 177, 182, 186, 207.

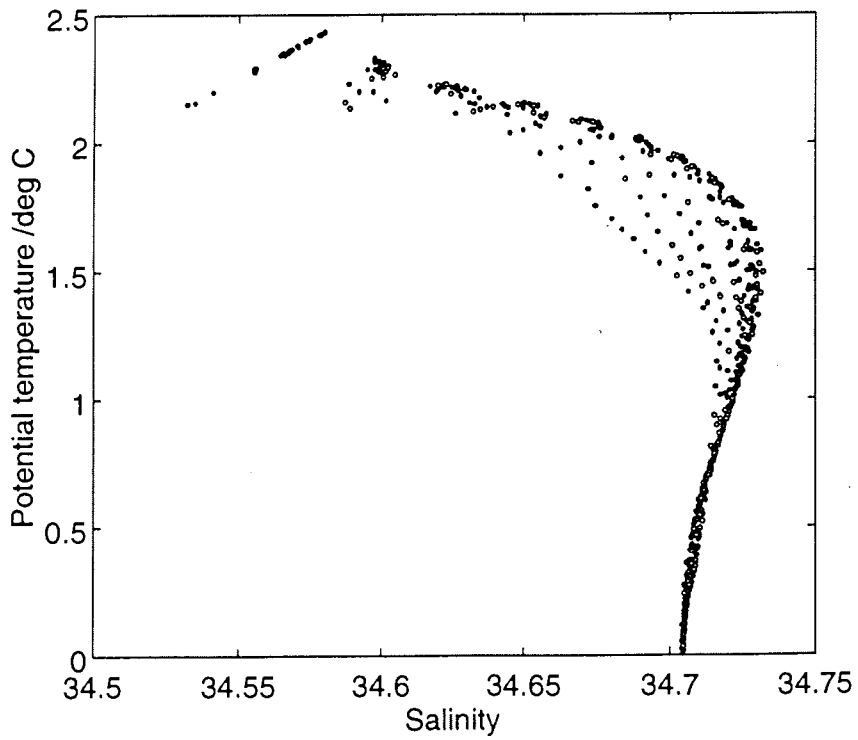

Figure 5. $\Theta - S$ diagram calculated for $\sigma_2 > \sigma_2^1 = 36.8\,kgm^{-3}$. Calculated for the stations: 14, 17, 19, 21, 23, 26, 28, 30, 32, 37, 45, 47, 55, 60, 138, 141, 154, 162, 166, 172, 177, 182, 186, 207.

7 References

McDougall, T.J., 1984: The Relative Roles of Diapycnal and Isopycnal Mixing on Subsurface Water Mass Conversion, *J. Phys. Oceanogr.*, 14, 1577-1589.

McDougall, T.J., 1987: Neutral Surfaces, *J. Phys. Oceanogr.*, 17, 1950-1964.